

**UNIVERSITA' VITA-SALUTE SAN RAFFAELE**  
**CORSO DI DOTTORATO DI RICERCA INTERNAZIONALE**  
**IN MEDICINA MOLECOLARE**

**Curriculum in Experimental and Clinical Medicine**

**QUANTITATIVE MULTIMODALITY**  
**IMAGING FOR THE CHARACTERIZATION**  
**OF MYOCARDIAL INFLAMMATORY**  
**DISEASES**

DoS: Prof. Antonio Esposito

Second Supervisor: Prof. Luca Saba

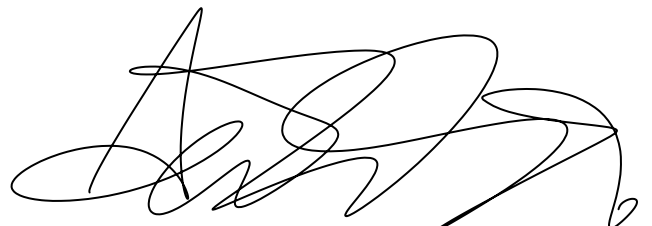
Tesi di DOTTORATO di RICERCA di Dott. Davide Vignale

matr. 017647

Ciclo di dottorato XXXVI

SSD MED/36

Anno Accademico 2022/2023

A handwritten signature in black ink, appearing to be 'Davide Vignale', located at the bottom right of the page.

## CONSULTAZIONE TESI DI DOTTORATO DI RICERCA

Il sottoscritto Davide Vignale  
Matricola/*registration number* 017647  
Nato a/ *born at* Alessandria (AL)  
il/*on* 30/06/1990

autore della tesi di Dottorato di ricerca dal titolo/*author of the PhD Thesis titled*

### QUANTITATIVE MULTIMODALITY IMAGING FOR THE CHARACTERIZATION OF MYOCARDIAL INFLAMMATORY DISEASES

- AUTORIZZA la Consultazione della tesi / *AUTHORIZES the public release of the thesis*  
 NON AUTORIZZA la Consultazione della tesi per 24 mesi / *DOES NOT AUTHORIZE the public release of the thesis for ..... months*

a partire dalla data di conseguimento del titolo e precisamente / *from the PhD thesis date, specifically*

Dal / *from* ...../...../..... Al / *to* ...../...../.....

Poiché /*because*:

- l'intera ricerca o parti di essa sono potenzialmente soggette a brevettabilità/ *The whole project or part of it might be subject to patentability;*
- ci sono parti di tesi che sono già state sottoposte a un editore o sono in attesa di pubblicazione/ *Parts of the thesis have been or are being submitted to a publisher or are in press;*
- la tesi è finanziata da enti esterni che vantano dei diritti su di esse e sulla loro pubblicazione/ *the thesis project is financed by external bodies that have rights over it and on its publication.*

E' fatto divieto di riprodurre, in tutto o in parte, quanto in essa contenuto / *Copyright the contents of the thesis in whole or in part is forbidden*

Data /*Date* 15/12/2023

Firma /*Signature* Davide Vignale



## **DECLARATION**

This thesis has been:

- composed by myself and has not been used in any previous application for a degree. Throughout the text I use both 'I' and 'We' interchangeably.
- written according to the editing guidelines approved by the University.

Permission to use images and other material covered by copyright has been sought and obtained.

All the results presented here were obtained by myself.

All sources of information are acknowledged by means of reference.

## ABSTRACT

### Background

Chronic myocardial inflammation is the substrate for arrhythmias and progression to dilated cardiomyopathy. Its identification and the prediction of adverse outcomes is crucial for guiding clinical management. Developing preclinical research platforms analogue to the clinical setting is fundamental for translational research.

### Aims

The aims are i) to develop multiparametric CMR-based models for prediction of prognosis in patients with chronic myocarditis and ii) to implement T1 mapping for the evaluation of mice model of experimental autoimmune myocarditis (EAM).

### Material and Methods

Clinical retrospective study on 93 patients (Male:Female=56:37; age 43 [IQR 32-53] years), with a diagnosis of chronic myocarditis based on clinical and imaging criteria, who underwent CMR for the assessment of fibrosis/necrosis and edema with qualitative (LGE and STIR), semiquantitative (scar burden and T2-ratio) and quantitative (T2, T1 and ECV mapping) parameters. These parameters were used to create prediction models for a long-term composite outcome of persistent symptoms, arrhythmias, ICD/PM implantation, and hospitalization. Preclinical study on 8 BALB/c mice subjected to EAM induction and 7T cardiac MRI (Bruker BioSpec 70/30) with pre- and post-contrast T1 mapping acquired with IG-FLASH Variable Flip Angle (VFA) sequence and reconstructed with DESPOT1 analysis (using a fitting algorithm to derive T1 and  $M_0$  from the slope and the intercept of the linearized Ernst equation).

### Results

34/93 (37%) patients had the composite outcome. A model based on extension of multiparametric CMR alterations and LV dysfunction reached fair predictability (AUC 0.717). In patients with active inflammation, a model based on the intensity of multiparametric alterations (T1, T2, ECV, T2-ratio and scar burden) and LV dysfunction had very good performance (AUC 0.850). Mice with EAM had significantly lower LV EF (54% [51-55] vs 60% [59-63],  $p=0.024$ ) and higher T1 (804 ms [780-863] vs 724 ms [722-725],  $p=0.222$ ). In mice with EAM, T1 significantly decreased after contrast injection (804 ms [780-863] vs 554 ms [443-586],  $p=0.016$ ).

### Conclusion

The quantitative multiparametric analysis of CMR biomarkers indicative of myocardial damage severity has very good predictive value in patients with chronic active myocarditis. In a preclinical EAM model, T1 mapping allows non-invasive tissue characterization and may be used in future longitudinal models.

## TABLE OF CONTENTS

ACRONYMS AND ABBREVIATIONS.....	3
LIST OF FIGURES AND TABLES.....	5
INTRODUCTION.....	6
Diagnosis.....	7
Prognostication with CMR .....	8
Preclinical imaging model of myocarditis.....	8
AIM OF THE WORK.....	10
RESULTS (AIM 1).....	11
Demographic and clinical features.....	11
Follow-up .....	13
Cardiac Magnetic Resonance findings .....	14
Comparison between patients experiencing or not the composite outcome....	17
Prediction of the composite outcome .....	21
DISCUSSION (AIM 1) .....	28
RESULTS (AIM 2).....	32
CMR experiments .....	32
Function and LGE.....	32
T1 mapping .....	33
DISCUSSION (AIM 2) .....	35
MATERIAL AND METHODS (AIM 1) .....	37
Study design and population .....	37
CMR acquisition protocol.....	38
CMR analysis.....	39
Endomyocardial biopsy and histological analysis .....	40
Study endpoint.....	40
Statistical analysis .....	41
MATERIAL AND METHODS (AIM 2) .....	42

Study design.....	42
Experimental autoimmune myocarditis induction .....	42
CMR acquisition protocol.....	42
CMR analysis.....	43
T1 quantification.....	43
Histopathological analysis .....	44
REFERENCES.....	45

## **ACRONYMS AND ABBREVIATIONS**

**AV:** Atrioventricular

**BSA:** Body Surface Area

**CFA:** Complete Freund's Adjuvant

**CI:** Confidence Interval

**ce-SSFP:** Contrast Enhanced Steady State Free Precession

**CMR:** Cardiac Magnetic Resonance

**CHF:** Chronic Heart Failure

**DCM:** Dilated Cardiomyopathy

**ECV:** Extracellular Volume Fraction

**EDV:** End-Diastolic Volume

**EDWM:** End-Diastolic Wall Mass

**ECG:** Electrocardiogram

**EF:** Ejection Fraction

**EMB:** Endomyocardial biopsy

**ESV:** End-Systolic Volume

**FA:** Flip Angle

**FLASH:** Fast Low-Angle Shot

**hsTnT:** high specificity Troponin T

**ICD:** Implantable Cardioverter-Defibrillator

**IG:** IntraGated

**IV:** Intraventricular

**LBBB:** Left Bundle Branch Block

**LGE:** Late Gadolinium Enhancement

**LLC:** Lake Louise Criteria

**LV:** Left Ventricle

**NSVT:** non-sustained ventricular tachycardia

**NT-proBNP:** N-terminal Pro Brain Natriuretic Peptide

**PB19:** Parvovirus B19

**PM:** Pace-Maker

**PVCs:** Premature Ventricular Contractions

**RBBB:** Right Bundle Branch Block

**RV:** Right Ventricle

**SA:** Short-Axis

**STIR:** Short Tau Inversion Recovery

**SVT:** Sustained Ventricular Tachycardia

**TE:** Echo Time

**TR:** Repetition Time

**VA:** Ventricular Arrhythmias

**VF:** Ventricular Fibrillation



## **LIST OF FIGURES AND TABLES**

*Table 1. Demographic and clinical features of the study population.*

*Table 2. Summary of outcomes at follow-up.*

*Table 3. CMR findings in the whole population.*

*Table 4. Demographic and clinical features stratified according to the outcome.*

*Table 5. CMR findings stratified according to the outcome.*

*Figure 1. ROC curve of the clinical model.*

*Figure 2. ROC curves of the standard CMR models.*

*Figure 3. ROC curves of the damage extension CMR model.*

*Figure 4. ROC curves of the damage intensity CMR model.*

*Figure 5. Post-contrast cine-IG-FLASH images in mice 40 days after EAM induction.*

*Figure 6. Acquisition of VFA cine-IG FLASH sequences.*

*Figure 7. Native T1 map.*

*Figure 8. Post-contrast T1 map.*

*Table 6. Correlations of variables used in the model.*

## **INTRODUCTION**

Myocarditis is a disease distinguished by inflammation that can arise after infections, immune system activation, or exposure to toxic substances (Cooper, 2009). The European Society of Cardiology (ESC) (Caforio *et al*, 2013) defines myocarditis as the evidence of inflammatory infiltrates in the myocardium associated with degeneration of myocytes and necrosis according to the Dallas criteria (Aretz, 1987).

Its clinical presentation is highly variable and ranges from almost asymptomatic forms to acute fulminant forms associated to unfavorable outcomes. Most cases of myocarditis heal spontaneously; however, in some patients, persistent inflammation of myocardium can lead to fibrosis and eventually to adverse left ventricle (LV) remodeling (Towbin *et al*, 2006) and consequent dilated cardiomyopathy (DCM) or non-dilated left ventricular cardiomyopathy (Arbelo *et al*, 2023).

Furthermore, extensive fibrosis and persistence of myocardial inflammation can cause electrical instability of the myocardium and consequent onset of life-threatening ventricular arrhythmias (Peretto *et al*, 2020).

Myocarditis prevalence is difficult to assess due to the difficulty in diagnosis caused by the heterogeneous clinical presentation. In adults with unexplained DCM, biopsy-proven myocarditis occurs in 9-16% of cases (Felker *et al*, 1999), while in the youngsters with sudden cardiac death, it has a reported prevalence of 2-42% (Basso *et al*, 2001; Corrado *et al*, 2001).

According to a report on the global incidence of cardiovascular diseases, the incidence of myocarditis ranges from 6.1 per 100.000 in males and 4.4 per 100.000 in females, with related mortality of 0.2 and 0.1 per 100.000, respectively (Roth *et al*, 2020).

Myocarditis can be classified according to different features such as etiology, phase, clinical presentation, symptoms, histology, and immunohistochemistry (Sagar *et al*, 2012; Ammirati *et al*, 2020).

Based on clinical presentation, acute myocarditis is diagnosed when the time between symptoms onset and diagnosis is short, usually less than one month. On the contrary, when the symptoms duration is more than one month, the term chronic

inflammatory cardiomyopathy can be used. This condition is usually associated to DCM or non-dilated left ventricular cardiomyopathy (Ammirati *et al*, 2020).

## **Diagnosis**

Endomyocardial biopsy (EMB) has always been considered the standard of reference for diagnosis, however has low sensitivity due to possible sampling error and inhomogeneous myocarditic involvement of the heart and is not free from complications (Bennett *et al*, 2013).

Thus, currently the non-invasive diagnosis of both acute and chronic myocarditis is reached based on imaging and clinical criteria. Currently, the non-invasive gold standard is CMR, thanks to its unparalleled capabilities of myocardial tissue characterization (Caforio *et al*, 2013).

The CMR diagnostic criteria for myocarditis have been established in 2009 with the so called Lake Louise Criteria (Friedrich *et al*, 2009), which allowed the diagnosis of myocarditis in presence of 2 out of 3 phenomena typical of inflammation, namely myocardial edema, hyperemia, and necrosis/fibrosis. These three phenomena had their CMR corresponding alteration as focal or diffuse hyperintensity on STIR images, hyperintensity in T1 images acquired immediately post-contrast administration, and late phase LGE in non-ischemic pattern (i.e., with subepicardial or mesocardial distribution).

However, due to their suboptimal performance (diagnostic accuracy around 80%) (Esposito *et al*, 2016), especially in chronic setting (Lagan *et al*, 2018), and the subsequent introduction of quantitative parametric mapping techniques (Hinojar *et al*, 2015), that allow microstructural quantitative evaluation of myocardium, LLC were updated in 2018 to include this novel techniques (Ferreira *et al*, 2018), which significantly increased their diagnostic performance (Luetkens *et al*, 2019).

Thus, nowadays myocarditis diagnosis is based on the identification of 2 out of 2 criteria:

- 1) T1 criteria: increase in native T1 or ECV values or presence of LGE with non-ischemic pattern
- 2) T2 criteria: increase in T2 values or presence of focal STIR hyperintensity or T2-ratio (ratio between the signal intensity of myocardium and skeletal muscle)  $\geq 1.9$ .

While in the acute setting their performance is now optimal, in the chronic setting the 2018 LLC criteria still have a reduced diagnostic performance due to the more subtle and diffuse nature of myocardial alterations (Lurz *et al*, 2016).

### **Prognostication with CMR**

Besides diagnosis, many studies have proposed CMR as a potent tool for risk stratification in inflammatory cardiomyopathies due to its extraordinary capabilities of non-invasive tissue characterization (Ferreira *et al*, 2018; Friedrich *et al*, 2009).

These studies, based on conventional techniques or mapping parameters, have identified many distinct CMR parameters capable of risk stratification, from indicators of LV systolic function (Sanguineti *et al*, 2015; Spieker *et al*, 2017; Ammirati *et al*, 2018), to presence and pattern of scar and necrosis evaluated with LGE (Grün *et al*, 2012; Greulich *et al*, 2020; Aquaro *et al*, 2017; Gräni *et al*, 2017), to presence and intensity of edema on STIR images (Gräni *et al*, 2017) and T2 mapping (Spieker *et al*, 2017).

However, studies evaluating the risk stratification capabilities of CMR in patients presenting long after previous myocarditis or new onset chronic myocarditis, which are commonly encountered in CMR practice, are scarce.

In fact, the few published studies are focused on a relatively short term (at maximum 1 year) CMR follow-up (Bohnen *et al*, 2017; Lurz *et al*, 2016; Luetkens *et al*, 2016; Radunski *et al*, 2017).

Thus, with this study we aim at filling this gap on knowledge.

### **Preclinical imaging model of myocarditis**

Preclinical models are fundamental for the understanding of molecular and cellular mechanism of inflammatory heart disease (Błyszczuk, 2019).

In particular, animal models can act as platform to study specific aspects of the diseases or to test pharmacological treatment that in the setting of myocarditis are currently lacking.

Animal models of myocarditis are usually classified according to the induction mechanism into infective and non-infective (i.e., autoimmune) (Błyszczuk, 2019).

EAM animal models may resemble more closely the pathophysiological progression from the acute phase to the chronic inflammatory phase, and thus are the more adapt

to parallel the design of our clinical study. Thus we aimed to create a model of EAM and to study it with high field multiparametric CMR.

## **AIM OF THE WORK**

The scope of this project was to develop novel approaches for the prognostication of inflammatory cardiomyopathies and to create a preclinical model of myocarditis that could be used for future longitudinal studies.

Therefore, specific aims were:

- 1) To create a prognostic model in the setting of chronic inflammatory cardiomyopathy based on a multiparametric CMR approach combining conventional parameters and novel mapping techniques.
  
- 2) To create a mouse model of EAM comprising a multiparametric evaluation with CMR.

## RESULTS (AIM 1)

### Demographic and clinical features

The ninety-three patients included in the study were mostly male (56/93, 60%) with a median age of 43 (interquartile range [IQR], 32 - 53) years. Thirty-four out of ninety-three (37%) patients had history of autoimmune diseases.

At the time of CMR, symptomatic patients were 26/93 (28%), mostly suffering from dyspnea (13/26, 50%) and chest pain (12/26, 46%); less patients reported palpitations (7/26, 27%). Among symptomatic patients, three out of twenty-six (12%) had a recent flu-like syndrome.

Fifty-two out of ninety-three (56%) of patients had ECG anomalies, mostly (32/52, 62%) premature ventricular contractions (PVCs) at standard or Holter ECG monitoring, while 21/52 (40%) patients had more than one ECG abnormality. Episodes of non-sustained ventricular tachycardia (NSVT) were documented in 8/93 (9%) patients.

Before CMR, 53/93 (57%) patients underwent transthoracic echocardiography, which highlighted wall motion alterations in 18/53 (34%) patients, with a median LV EF of 60 (IQR, 55-60) %.

At the time of CMR, high specificity troponin T (hsTnT) was evaluated in 77/93 (83%) patients, with a median value of 11 (IQR, 5 - 37) ng/L (normal values < 14 ng/L). hsTnT resulted elevated in 35/77 (45%) patients, with a median value of 51 (IQR, 27 - 130) ng/L.

Nineteen out of 93 (20%) of patients did not have symptoms, alterations of ECG, arrhythmias, wall motion abnormalities at echocardiography, nor hsTnT elevation, but had received a previous diagnosis of myocarditis based on clinical and imaging criteria.

EMB was performed in 58/93 (62%) patient, with positive findings in 45/58 (78%) samples. In patients with negative EMB, negativity was attributable to sampling error.

Demographic and clinical feature are reported in Table 1.

Table 1. Demographic and clinical features of the study population.

<b>Clinical and demographic characteristics (n = 93)</b>	
Male, n (%)	56 (60)
Age, years (IQR)	43 (32 - 53)

Autoimmunity, n (%)	34 (37)
<b>Symptoms (n = 93)</b>	
Dyspnea, n (%)	13 (14)
Chest pain, n (%)	12 (13)
Palpitations, n (%)	7 (8)
Asymptomatic, n (%)	67 (72)
<b>ECG (n = 93)</b>	
ECG alterations, n (%)	52 (56)
AV conduction disorders, n (%):	4 (4)
- First degree AV block, n (%)	3 (3)
- Sinus arrest, n (%)	1 (1)
IV conduction disorders, n (%):	10 (11)
- LBBB, n (%)	3 (3)
- RBBB, n (%)	7 (8)
Supraventricular ectopic activity, n (%)	15 (16)
PVCs, n (%)	32 (34)
NSVT, n (%)	12 (13)
Repolarization abnormalities, n (%):	8 (9)
- Nonspecific ST-T alterations, n (%)	6 (6)
- Q waves, n (%)	2 (2)
Brugada Pattern 1, n (%)	1 (1)
<b>Transthoracic Echocardiography (n = 53)</b>	
LV regional wall motion abnormalities, n (%):	18 (34)



- Inferior wall, n (%)	6 (11)
- Apex, n (%)	2 (4)
- Interventricular septum, n (%)	4 (8)
- Lateral wall, n (%)	2 (4)
- Global LV hypokinesia, n (%)	7 (13)
Pericardial effusion	2 (4)
EF, % (IQR)	60 (55 – 60)
<b>Cardiac biomarkers</b>	
hsTnT, ng/L (IQR), n = 77	11 (5 – 37)
NT-ProBNP, pg/mL (IQR), n = 49	74 (23 - 150)
<b>Endomyocardial biopsy (n = 58)</b>	
Chronic active lymphocytic myocarditis, n (%)	42 (57)
- PB19 positive, n (%)	6 (10)
- Virus negative, n (%)	36 (62)
Aspecific inflammatory cardiomyopathy	3 (5)
Myocardial fibrosis, n (%)	3 (5)
Aspecific findings, n (%)	2 (3)
Negative, n (%)	7 (12)
Non diagnostic, n (%)	1 (2)

### Follow-up

After a median of 21 (17 – 35) months we collected the follow-up. The composite outcome occurred in 34/93 (37%) patients. In detail, no patients suffered from cardiovascular death, four out of ninety-three (4%) patients received a diagnosis of CHF due to presence of dyspnea and chronically elevated levels of NT-proBPN (329,

1005, 207, and 449 pg/mL, cut-off for CHF diagnosis: >125 pg/mL (Bozkurt *et al*, 2021)), six out of ninety-three patients (6%) patients had hospitalizations for cardiac reasons, nine out of ninety-three (10%) patients had recurrent chronic myocarditic chest pain, seven out of ninety-three (8%) patients had ICD/PM implantation, 20/93 (22%) had arrhythmias, most frequently (11/23, 48%) PVCs with Lown grade >2 (Bastiaenen *et al*, 2012). Some patients experienced multiple outcomes (Table 2).

Table 2. Summary of outcomes at follow-up.

Composite outcome reached, n (%):	34 (37)
- CHF, n (%) (IQR)	4 (4)
- Hospitalization for cardiac reasons, n (%)	6 (6)
- Recurrent chronic myocarditic chest pain, n (%)	9 (10)
- ICD/PM implantation, n (%)	7 (8)
- Chest pain, n (%)	9 (10)
- VAs, n (%):	20 (22)
o High grade AV block, n (%)	1 (1)
o NSVT, n (%)	3 (3)
o SVT, n (%)	1 (1)
o PVCs, n (%):	11 (12)
▪ Lown grade 2	7 (8)
▪ Lown grade 4a	2 (2)
▪ Lown grade 4b	2 (2)

### Cardiac Magnetic Resonance findings

In the overall population, LV and RV volume and function were preserved in most cases. Six out of ninety-three patients had reduced LVEF (<50%), with median values of 40 (37 - 48%); all these patients experienced the composite outcome, with one of them developing CHF and VAs, one CHF, one recurrent myocarditic chest pain and

hospitalization for cardiac reasons, one ICD implantation and VAs, two ICD implantation, and one VAs.

Only one male patient presented with LV dilation (EDV/BSA 115 mL/m<sup>2</sup>, normal value < 110 mL/m<sup>2</sup> (Petersen *et al*, 2017)) and he reached the outcome of ICD implantation.

At least one CMR abnormality was found in all patients.

Focal edema on STIR sequences was present only in 42/93 (45%) patients, mostly with a transmural and subepicardial pattern, while LGE was present in 83/93 (89%) patients with a predominant subepicardial distribution (58/83, 70%).

Native and post-contrast T1 mapping were not assessable in one (1%) and two (2%) patients, respectively, due to breathing artifacts; in the remaining patients, native T1 mapping was assessable in 1394/1472 (95%) segments, while ECV was assessable in 1374/1456 (94%) segments.

T2 mapping was not assessable in one (1%) patient. In the remaining patients, T2 mapping was assessable in 1394/1472 (95%) segments.

In the whole population, global native T1 values, ECV values, and T2 values were at the higher limit of center-specific ranges (native T1: 1040 [1020-1078] ms, v.n. < 1045 ms; ECV: 26.8 (24.4 – 29.5) %, v.n. ≤ 27.0%; T2: 50 (48 – 52) ms, v.n. < 53 ms).

The median percentage of altered segments was 41 (11 – 83) % for native T1 mapping, 44 (8 – 84) % for ECV, and 19 (0 - 44) % for T2 mapping.

2009 LLC were positive in 76/93 (82%) of patients, while 2018 LLC in 85/93 (91%) patients (p=0.008). All the eight patients with negative 2018 LLC had history of previous myocarditis and had at least one segment involved by LGE with myocarditic distribution, and were thus diagnosed with previous myocarditis. However, three of them were symptomatic (one for dyspnea, one for dyspnea and chest pain, one for palpitations).

CMR results are summarized in table 3.

*Table 3. CMR findings in the whole population.*

<b>Volumes and function (n = 93)</b>	
LV-EDV, mL (IQR)	136 (113 – 153)
LV-EDV indexed, mL/m <sup>2</sup> (IQR)	73 (65 – 80)
LV-EDWM, g (IQR)	92 (76 – 108)

LV-EDWM indexed, g/m <sup>2</sup> (IQR)	48 (42 – 55)
LV-EF (%) (IQR)	60 (55 – 67)
RV-EDV, mL (IQR)	135 (112 – 156)
RV-EDV indexed, mL/m <sup>2</sup> (IQR)	71 (61 – 79)
RV-EF (%) (IQR)	59 (52 – 63)
<b>STIR (n = 93)</b>	
Patients with positive STIR, n (%)	42 (45)
Segments involved in positive patients, n (IQR)	2 (1 – 4)
T2-ratio (IQR)	2.0 (1.9 – 2.3)
<b>LGE (n = 93)</b>	
Patients with positive LGE, n (%)	83 (89)
Segments involved in positive patients, n (IQR)	4 (2 – 6)
Scar burden 5DS, % (IQR)	2.6 (1.2 – 5.3)
<b>Native T1 mapping (n = 92)</b>	
Global value, ms (IQR)	1040 (1020 – 1078)
Percentage of altered segments, % (IQR)	41 (11 – 83)
<b>T2 mapping (n = 92)</b>	
Global value, ms (IQR)	50 (48 – 52)
Percentage of altered segments, % (IQR)	19 (0 – 44)
<b>ECV (n = 91)</b>	
Global value, ms (IQR)	26.8 (24.4 – 29.5)
Percentage of altered segments, % (IQR)	44 (8 – 48)
<b>LLC criteria</b>	

Positive 2009 LLC, n (%)	76 (82)
Positive 2018 LLC, n (%)	85 (91)

### Comparison between patients experiencing or not the composite outcome

The demographic data of patients that reached or not the composite outcome was not significantly different, as well as the symptoms at presentation. However, patients experiencing the outcome had more frequently ECG alterations (84% vs 41%,  $p < 0.001$ ) than patients who did not, driven by the higher frequency of PVCs in the former population (59% vs 22%,  $p < 0.001$ ). Interestingly, no statistically significant differences were noted regarding the frequency of NSVT (21% vs 8%,  $p = 0.115$ ), although with a tendency towards higher rate in patients experiencing the outcome.

No differences were noted for echocardiographic and biomarkers alterations at presentation.

Interestingly, EMB was more frequently performed in patients experiencing the outcome at long term (84% vs 41%,  $p = 0.010$ ), but the positivity rate was higher in those patients who did not reach the outcome (84% vs 59%,  $p = 0.045$ ).

Detailed demographic and clinical features stratified according to the outcome are reported in table 4.

Table 4. Demographic and clinical features stratified according to the outcome.

Variable	Outcome	No outcome	p-value
<b>Clinical and demographic characteristics (n = 93)</b>			
Male, n (%)	20 (59)	36 (61)	0.835
Age, years (IQR)	45 (33-53)	40 (29-53)	0.382
Autoimmunity, n (%)	12 (38)	22 (40)	0.818
<b>Symptoms (n = 93)</b>			
Dyspnea, n (%)	5 (15)	8 (14)	0.878
Chest pain, n (%)	6 (18)	6 (10)	0.300
Palpitations, n (%)	4 (12)	3 (5)	0.254

Asymptomatic, n (%)	21 (62)	46 (78)	0.094
<b>ECG (n = 93)</b>			
ECG alterations, n (%)	27 (84)	24 (41)	<b>&lt;0.001</b>
AV conduction disorders, n (%):	3 (9)	1 (2)	0.137
- First degree AV block, n (%)	2 (6)	1 (2)	0.552
- Sinus arrest, n (%)	1 (3)	0 (0)	0.366
IV conduction disorders, n (%):	5 (15)	5 (8)	0.489
- LBBB, n (%)	1 (3)	2 (3)	1.000
- RBBB, n (%)	4 (12)	3 (5)	0.254
Supraventricular ectopic activity, n (%)	9 (26)	6 (11)	0.076
PVCs, n (%)	20 (59)	12 (22)	<b>&lt;0.001</b>
NSVT, n (%)	7 (21)	5 (8)	0.115
Repolarization abnormalities, n (%):	5 (15)	3 (5)	0.137
- Nonspecific ST-T alterations, n (%)	3 (9)	3 (5)	0.665
- Q waves, n (%)	2 (6)	0 (0)	0.131
Brugada Pattern 1, n (%)	0 (0)	1 (2)	1.000
<b>Transthoracic Echocardiography (n = 53)</b>			
LV regional wall motion abnormalities, n (%):	12 (39)	6 (22)	0.176
- Inferior wall, n (%)	4 (14)	2 (8)	0.678
- Apex, n (%)	2 (7)	0 (0)	0.495
- Interventricular septum, n (%)	4 (14)	0 (0)	0.117
- Lateral wall, n (%)	1 (3)	1 (4)	1.000

- Global LV hypokinesia, n (%)	3 (10)	4 (17)	0.688
Pericardial effusion	1 (3)	1 (4)	1.000
EF, % (IQR)	60 (51-60)	60 (55-62)	0.413
<b>Cardiac biomarkers</b>			
hsTnT, ng/L (IQR), n = 77	12 (5-36)	11 (5-51)	0.800
NT-ProBNP, pg/mL (IQR), n = 49	93 (30-275)	67 (22-127)	0.427
<b>Endomyocardial biopsy (n = 58)</b>			
EMB performed, n (%)	27 (79)	31 (53)	<b>0.010</b>
Chronic active lymphocytic myocarditis, n (%)	16 (59)	26 (84)	<b>0.045</b>
- PB19 positive, n (%)	2 (7)	4 (13)	0.675
- Virus negative, n (%)	14 (52)	22 (71)	0.178
Aspecific inflammatory cardiomyopathy	2 (7)	1 (3)	0.593
Myocardial fibrosis, n (%)	3 (11)	0 (0)	0.095
Aspecific findings, n (%)	2 (7)	0 (0)	0.212
Negative, n (%)	4 (15)	3 (10)	0.694
Non diagnostic, n (%)	0 (0)	1 (3)	1.000

At CMR, the only significant differences between patients reaching or not the composite outcome were in LV EF, which was significantly lower in the former group of patients (57 [51 – 61] vs 62 [57 – 68] %,  $p < 0.001$ ) and in the extent and intensity of edema in the STIR sequences, with higher number of positive segments and Higher T2 ratio in the former group (3 [2 – 14] vs 1 [1 – 2],  $p = 0.007$ , and 2.2 [2.0 – 2.3] vs 1.9 [1.8 – 2.1],  $p = 0.002$ ).

However, native T1 mapping, T2 mapping, and ECV showed a tendency towards higher values in patients experiencing the outcome, despite not reaching statistical significance. The same trend was evident for the percentage of altered segments for each mapping parameter.

LGE was not different between the two groups neither when analyzing the number of segments involved nor when evaluating the scar burden.

Detailed CMR data stratified according to the outcome are reported in table 5.

Table 5. CMR findings stratified according to the outcome.

Variable	Outcome	No outcome	p-value
<b>Volumes and function (n = 93)</b>			
LV-EDV, mL (IQR)	141 (118-149)	129 (109-153)	0.298
LV-EDV indexed, mL/m <sup>2</sup> (IQR)	74 (66-84)	71 (64-77)	0.114
LV-EDWM, g (IQR)	91 (75-112)	92 (76-108)	0.750
LV-EDWM indexed, g/m <sup>2</sup> (IQR)	48 (43-55)	49 (42-54)	0.675
LV-EF (%) (IQR)	57 (51-61)	62 (57-68)	<b>&lt;0.001</b>
RV-EDV, mL (IQR)	126 (101-151)	138 (112-159)	0.266
RV-EDV indexed, mL/m <sup>2</sup> (IQR)	70 (60-78)	72 (64-83)	0.208
RV-EF (%) (IQR)	59 (52-63)	60 (52-64)	0.404
<b>STIR (n = 93)</b>			
Patients with positive STIR, n (%)	14 (41)	28 (47)	0.558
Segments involved in positive patients, n (IQR)	3 (2-14)	1 (1-2)	<b>0.007</b>
T2-ratio (IQR)	2.2 (2.0-2.3)	1.9 (1.8-2.1)	<b>0.003</b>
<b>LGE (n = 93)</b>			
Patients with positive LGE, n (%)	30 (88)	53 (90)	1.000
Segments involved in positive patients, n (IQR)	5 (3-7)	4 (2-6)	0.226
Scar burden 5DS, % (IQR)	3.3 (1.0-7.0)	2.2 (1.2-5.0)	0.490
<b>Native T1 mapping (n = 92)</b>			



Global value, ms (IQR)	1064 (1026-1089)	1035 (1010-1069)	0.072
Percentage of altered segments, % (IQR)	75 (13-94)	31 (6-77)	0.064
<b>T2 mapping (n = 92)</b>			
Global value, ms (IQR)	51 (48-53)	50 (48-51)	0.211
Percentage of altered segments, % (IQR)	28 (8-56)	13 (0-36)	0.144
<b>ECV (n = 91)</b>			
Global value, ms (IQR)	27.7 (25.5-30.5)	26.6 (24.3-29.4)	0.142
Percentage of altered segments, % (IQR)	58 (19-77)	38 (7-88)	0.379
<b>LLC criteria</b>			
Positive 2009 LLC, n (%)	29 (85)	47 (80)	0.498
Positive 2018 LLC, n (%)	32 (94)	53 (90)	0.478

### **Prediction of the composite outcome**

To predict the composite outcome, we created several models based on clinical and CMR parameters and evaluated their performance by means of ROC curve analysis.

In particular, we created four different prediction models:

- 1) Clinical model: in this analysis, we used the most significant clinical parameters potentially available before CMR examination.
- 2) Standard CMR models: in this analysis, we created a model based on LLC positivity and a model using currently recognized and validated imaging parameters with prognostication capabilities, namely presence of LGE and LV EF.
- 3) Damage extension model: in this analysis, we used the segmental extension of edema on STIR images, LGE, and mapping parameters alterations.
- 4) Damage intensity model: in this analysis, we included only the patients with alterations of T1, T2 and ECV. We thus created a model using the intensity of

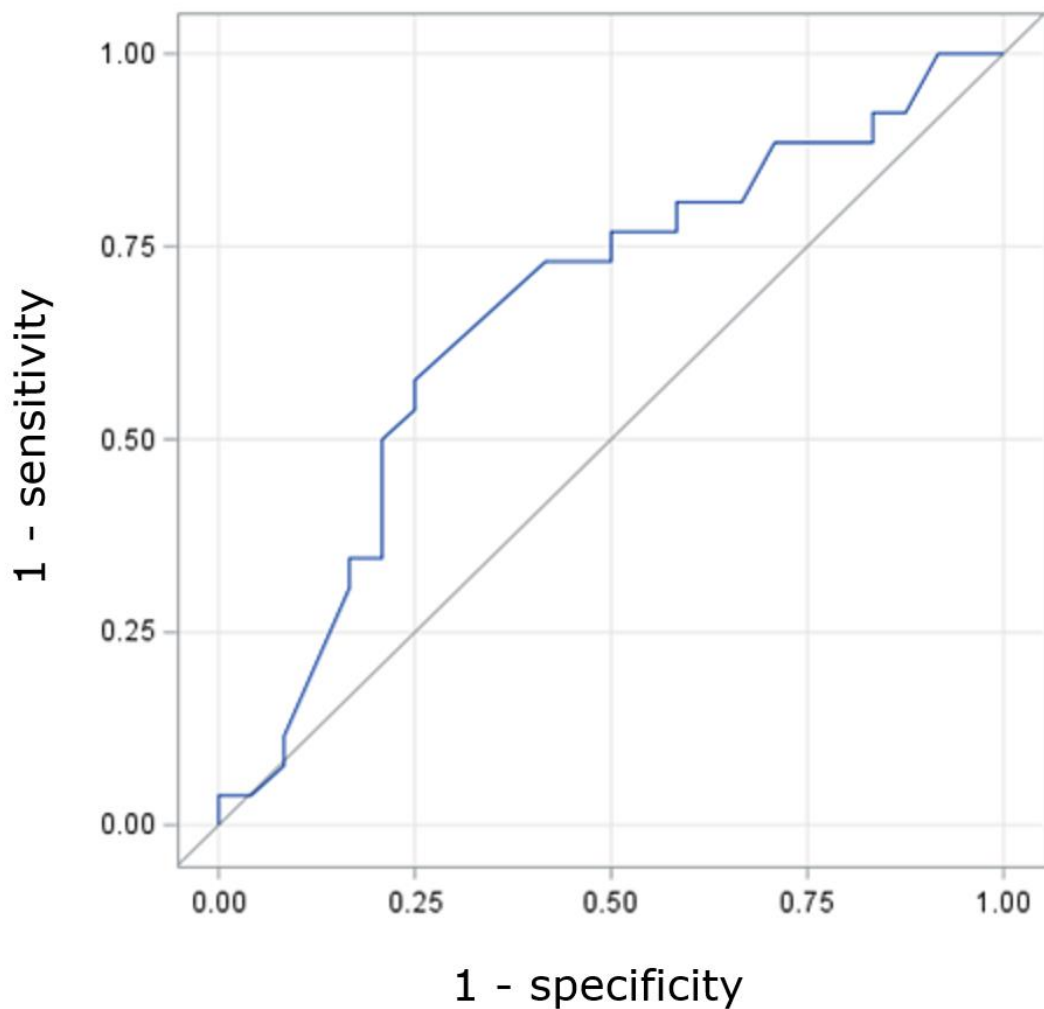
edema on STIR images, namely T2-ratio, the scar burden on LGE images, and the degree of alteration of mapping parameters.

The final aim was to create a multiparametric model capable of providing more prognostic information than the sole clinical information or the standard CMR evaluation based on LV EF and presence of LGE.

### **Clinical model**

To build the clinical model, we used three parameters: i) presence of symptoms, ii) presence of ECG anomalies, and iii) echocardiography-derived EF. The clinical model showed a fair capability of predicting the outcome, with an AUC of 0.667 (95% CI: 0.512 – 0.822) (Figure 1).

*Figure 1. ROC curve of the clinical model.*

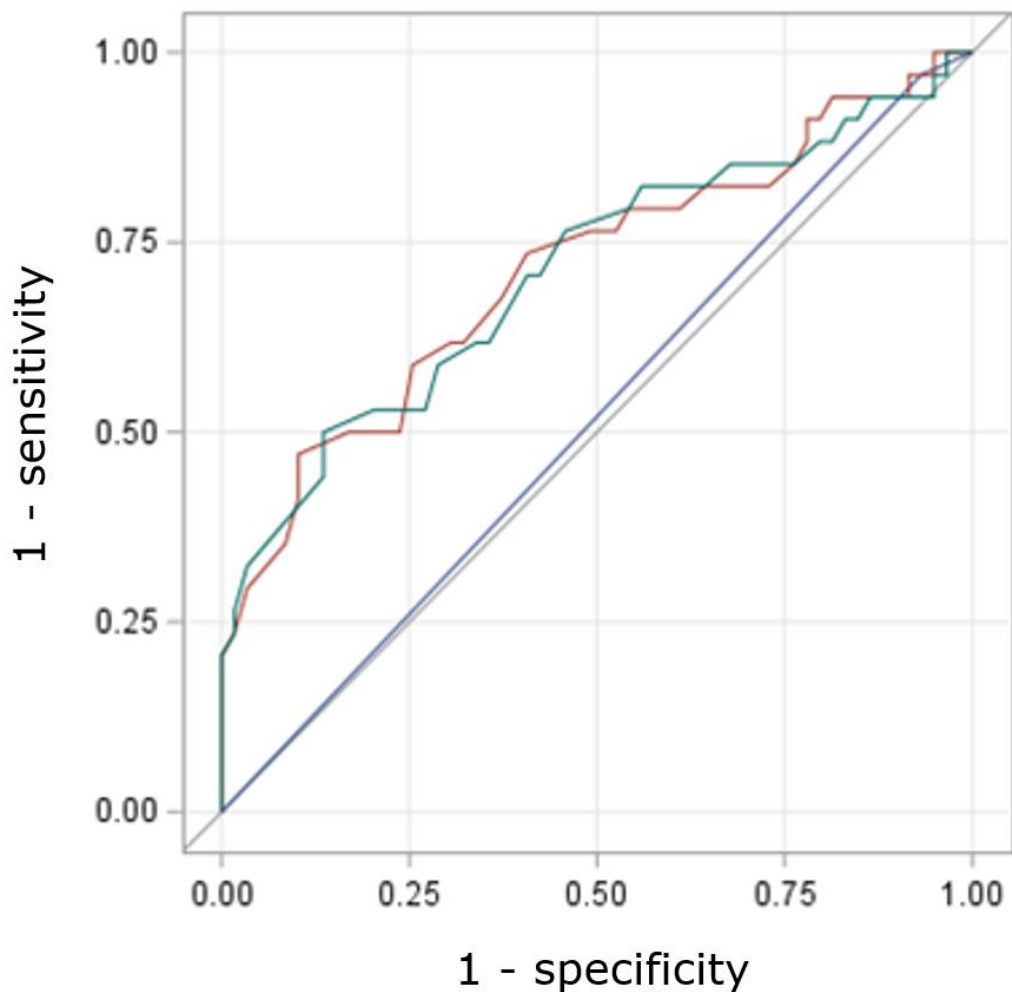


### **Standard CMR models**

In this analysis, we firstly created a model based on 2018 LLC positivity, which showed no capabilities of prognostication (blue line in figure 2, AUC: 0.519 [95% CI: 0.476 – 0.563]). Secondly, we created a model based on well recognized predictors of prognosis in the setting of cardiomyopathies of both inflammatory and non-inflammatory etiology, namely LV EF and presence/absence of LGE, which reached a fair performance (green line in figure 2, AUC of: 0.711 [95% CI: 0.594 – 0.827], significantly better than the model based on LLC positivity ( $p=0.003$ ).

However, the addition of LV EF to the LLC positivity model significantly increased its performance (red line in figure 2, AUC: 0.713 [95% CI: 0.597 – 0.828]), which became comparable to the LGE + LV EF model ( $p=0.904$ ), highlighting that the most important “classical” parameter of the CMR evaluation is the reduced EF.

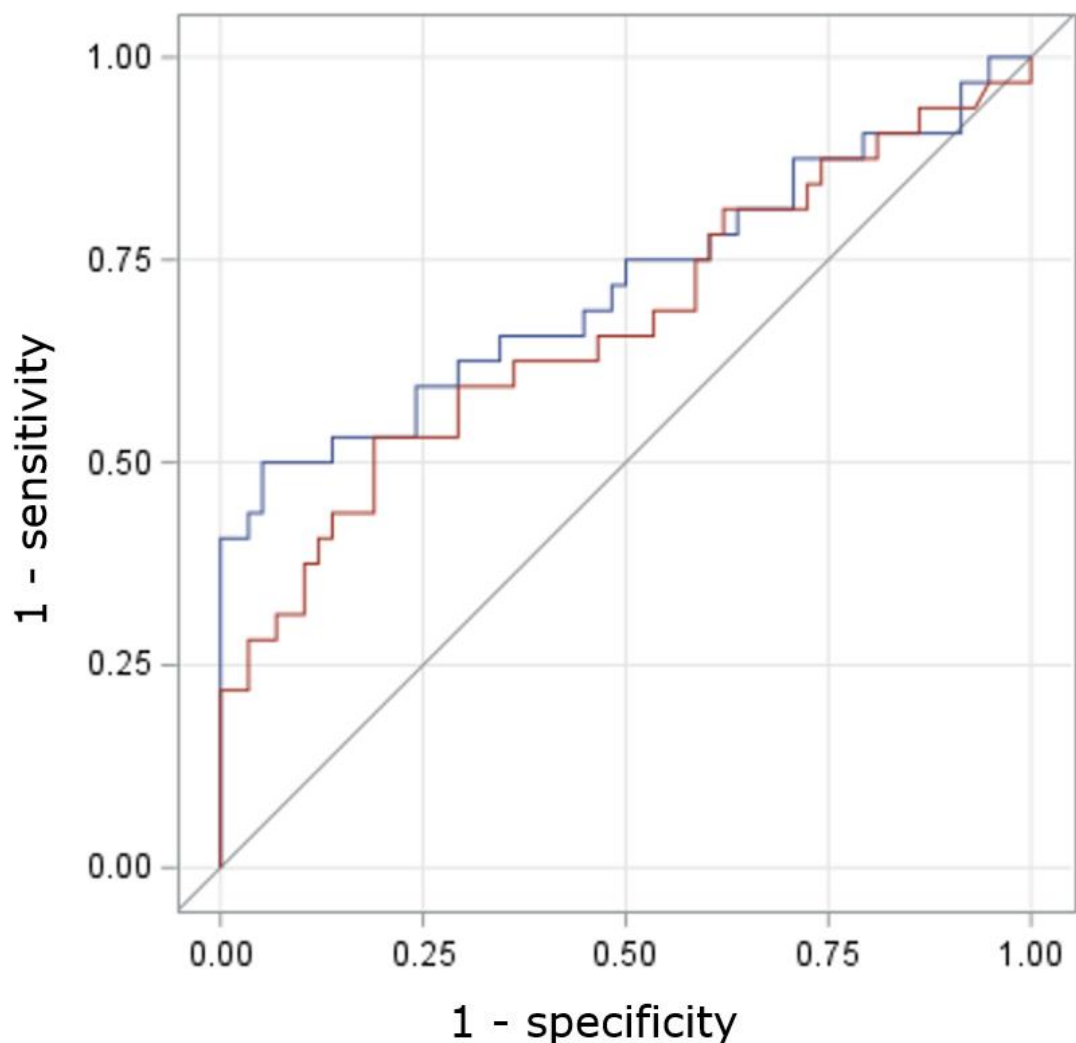
*Figure 2. ROC curves of the standard CMR models.*



### ***Damage extension model***

With this model we studied the role of myocardial damage extension through a quantitative evaluation of the myocardial segments with alterations. The model included qualitative and quantitative parameters of fibrosis (number of segments with LGE, percentage of segments with altered native T1 mapping and altered ECV), qualitative and quantitative parameters of edema (percentage of segments positive at STIR, number of segments with altered native T1 mapping and ECV). This model reached a fair prognostic capability, comparable to the clinical model (red line in figure 3, AUC: 0.669 [95% CI: 0.544 – 0.794]). Furthermore, when adding LV EF to the model, its performance slightly improved (blue line in figure 3, AUC: 0.717 (95% CI: 0.594 – 0.840) although it was not statistically significantly ( $p=0.297$ ).

*Figure 3. ROC curves of the damage extension CMR model.*

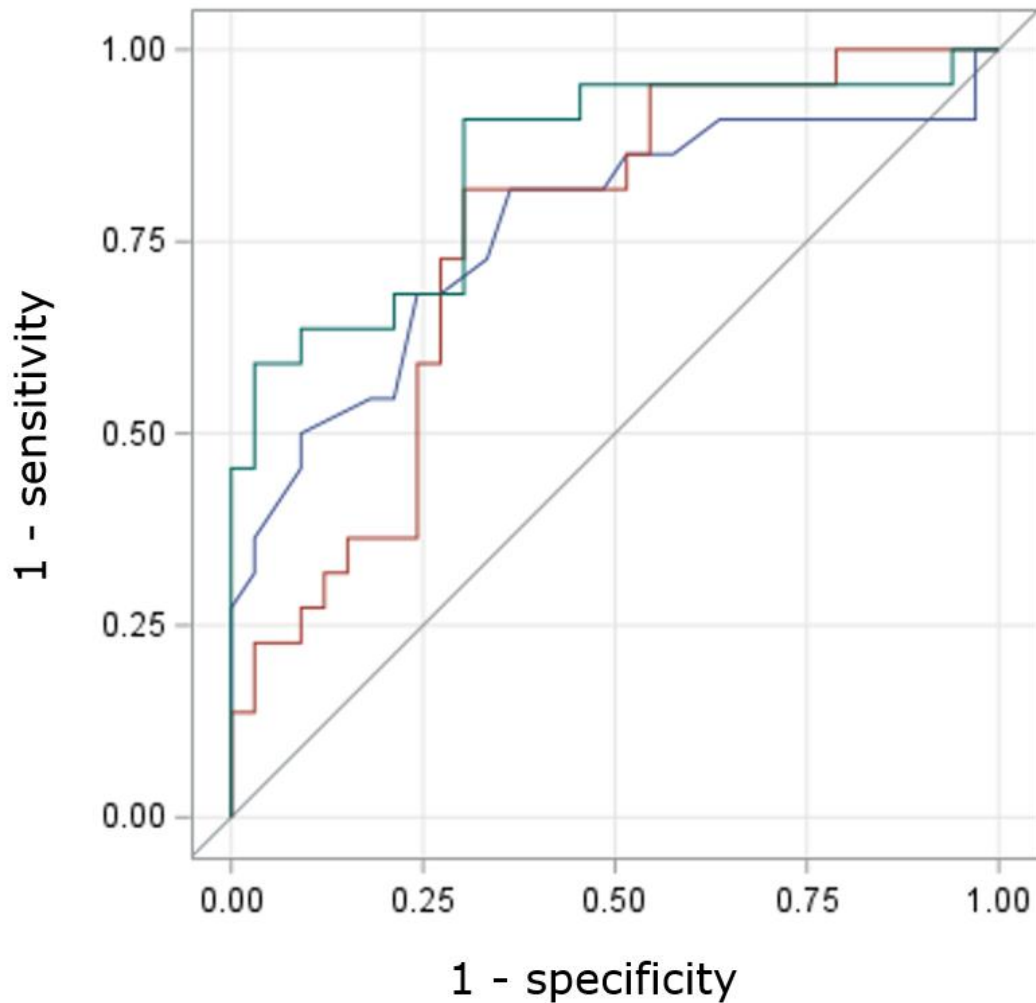


### ***Damage intensity model***

In this model we included only the 55 patients with alterations of T1, T2, and ECV. Among them, 22 (40%) reached the composite outcome. Since T2 mapping is specific for myocardial edema, we considered these patients to have active myocarditis. Instead of the extension of myocardial alteration, the model included the intensity of the alterations, thus we considered the mean value of native T1, T2, and ECV of the altered segments, the scar burden on LGE measured with a threshold of +5SD, and the mean of global T2-STIR ratio. This model reached a good prognostic capability (red line in figure 4, AUC: 0.752 [95% CI: 0.622 – 0.882]), comparable to that of a model including LV EF and LGE in this population (blue line in figure 4, AUC: 0.767 [95% CI: 0.629 – 0.906]).

However, when adding the LV EF to the damage intensity model, its classification capability increases to very good (green line in figure 4, AUC: 0.850 [95% CI: 0.740 – 0.960]), although this increase does not reaching statistical significance ( $p=0.109$ ) due to the relatively small number of patients.

Figure 4. ROC curves of the damage intensity CMR model.



In this model, the parameters that showed a significant association to the outcome were an increased native T1 mapping, indicative of necrosis, fibrosis, and edema, and a decreased LV EF, with odds ratio of 1.035 per 1 ms increase (95% CI: 1.002 – 1.070,  $p=0.039$ ) and 0.856 per 1% increase (95% CI: 0.770 – 0.952,  $p=0.004$ ), respectively (table 6).

Table 5. Odds ratio of the damage intensity model

Parameter	OR (95% CI)
Mean native T1 of altered segments	1.035 (1.002 - 1.070)

Mean T2 of altered segments	0.788 (0.520 - 1.195)
Mean ECV of altered segments	1.017 (0.776 - 1.332)
Scar burden (method 5DS)	0.992 (0.848 - 1.161)
Global T2 ratio	8.894 (0.813 - 97.307)
LV EF	0.856 (0.770 - 0.952)

All the parameters that were used in the models showed mild reciprocal correlation, reflecting their capability of depicting overlapping pathophysiological properties, thus no significant multicollinearity bias was present (table 6).

Table 6. Correlations of variables used in the model.

	Number of STIR positive segments	Number of LGE positive segments	Scar burden (5DS)	Global native T1	Global T2	Global ECV
Number of STIR positive segments		r=0.048 p=0.647	r=0.084 p=0.425	r=-0.049 p=0.641	r=0.156 p=0.137	r=0.084 p=0.427
Number of LGE positive segments	r=0.048 p=0.647		r=0.688 p<0.001	r=-0.077 p=0.467	r=-0.113 p=0.282	r=-0.72 p=0.497
Scar burden (5DS)	r=0.084 p=0.425	r=0.688 p<0.001		r=-0.155 p=0.139	r=-0.172 p=0.102	r=-0.063 p=0.553
Global native T1	r=-0.049 p=0.641	r=-0.077 p=0.467	r=-0.155 p=0.139		r=0.645 p<0.001	r=0.626 p<0.001
Global T2	r=0.156 p=0.137	r=-0.172 p=0.102	r=-0.172 p=0.102	r=0.645 p<0.001		r=0.539 p<0.001
Global ECV	r=0.084 p=0.427	r=-0.72 p=0.497	r=-0.063 p=0.553	r=0.626 p<0.001	r=0.539 p<0.001	

## **DISCUSSION (AIM 1)**

Myocarditis is a well-known significant contributor to mortality and morbidity, especially in the youngster (Eckart *et al*, 2011). However, due to heterogeneous clinical presentation and complex diagnostic process, it may be overlooked by clinicians (Caforio *et al*, 2017; Cooper & Fairweather, 2013).

In many cases, acute myocarditis has a favorable course towards resolution. However, in a portion of patients that some authors postulate could even be around 50% (Eichhorn *et al*, 2022), inflammation may become chronic, leading to progressive LV adverse remodeling with dilation and fibrosis causing heart failure and ventricular arrhythmias (Caforio *et al*, 2013).

Besides arising as the chronicization of an acute process, chronic myocarditis can also have a more subtle onset in the setting of patients with autoimmunity and autoimmune diseases (Caforio *et al*, 2017).

When evaluating a patient with evidence of previous myocarditis or chronic active myocarditis, an accurate risk stratification tool would be pivotal to tailor treatment and avoid adverse outcome (De Luca *et al*, 2020), in particular when choosing if to start an immunomodulatory drug (Tschöpe *et al*, 2021).

CMR, for its unparalleled capabilities of tissue characterization, is the modality of choice for the evaluation of inflammatory cardiomyopathies (Ferreira *et al*, 2018; Friedrich *et al*, 2009) and it's a strong candidate to become the tool for risk stratification in this setting. In fact, the prognostic capabilities of other strategies have proven limited. For example, laboratory markers of myocardial damage have no correlation to the prognosis (Ammann *et al*, 2003; Maron *et al*, 2015), while EMB, despite having strong prognostic capabilities (Kuethe *et al*, 2017; Kindermann *et al*, 2008), is hampered by invasiveness and high rate of false negatives due to sampling errors.

Thus, many studies have investigated the role of CMR for risk stratification in the acute setting, both with conventional techniques and mapping parameters, highlighting that LV EF (Sanguineti *et al*, 2015; Spieker *et al*, 2017; Ammirati *et al*, 2018), LGE presence (Grün *et al*, 2012; Greulich *et al*, 2020) and pattern (Aquaro *et*



*al*, 2017; Gräni *et al*, 2017), edema on STIR images (Gräni *et al*, 2017), and T2 mapping (Spieker *et al*, 2017) are predictors of adverse long term outcome.

However, studies evaluating the risk stratification capabilities of CMR in patients presenting long after previous myocarditis or new onset chronic myocarditis, which are a commonly encountered in CMR practice, are scarce.

In fact, the few published studies are focused on a relatively short term (at maximum 1 year) CMR follow-up (Bohnen *et al*, 2017; Lurz *et al*, 2016; Luetkens *et al*, 2016; Radunski *et al*, 2017).

Thus, to fill this gap in knowledge, we retrospectively enrolled 93 patients with known previous myocarditis or chronic active myocarditis, in order to identify CMR-derived parameters that could help the risk stratification of these patients.

The main findings of our study are:

- 1) 2018 LLC have found signs of active inflammation in a significantly high proportion of patients in our cohort, with superior performance in comparison to 2009 LLC.
- 2) A model based on a combination of clinical features has low predictive capabilities for adverse outcome (AUC 0.667)
- 3) A multiparametric CMR-based evaluation of fibrotic, necrotic and edematous areas extension, together with LV systolic function, has a fair capability of discriminating patients with future adverse outcome (AUC 0.717)
- 4) In patients with active inflammation demonstrated with T2 mapping, a multiparametric evaluation of the intensity of fibrosis, necrosis and edema, together with LV systolic function, has a very good performance in risk stratification (AUC 0.850)

In our cohort we confirmed that 2018 LLC have significantly higher sensitivity than 2009 LLC for myocardial inflammation, in agreement with previous reports (Luetkens *et al*, 2019).

We have also found a higher diagnostic performance of CMR in comparison to the one reported in a previous study with a similar setting (Lurz *et al*, 2016), in which the best parameter for the diagnosis of chronic myocarditis was T2 mapping with an AUC of 0.77. However, Lurz *et al*. used EMB as the gold standard, thus introducing bias due to possible sampling error and false negative results.

Regarding prognostication, it is known that clinical parameters alone, such as biomarkers of myocardial damage (Ammann et al, 2003; Maron et al, 2015), are not sufficiently accurate.

In the chronic setting, no studies have evaluated the prognostic value of ECG alteration presence. However, data coming from the setting of acute myocarditis suggest that ECG alterations may predict both a positive or negative course of disease (Imazio & Trinchero, 2008; Guidelines for diagnosis and treatment of myocarditis (JCS 2009): digest version., 2011), while the presence of ventricular arrhythmias may predict occurrence of future major arrhythmic events (Anzini *et al*, 2016). Thus, it is not surprising that also in our study in the chronic setting, a clinical model based on clinical features and ECG alterations is not accurate for risk stratification.

Surprisingly, the extension of myocardial necrosis and fibrosis or edema, assessed semiquantitatively with LGE and STIR and quantitatively with ECV, native T1 mapping, and T2 mapping, respectively, reached a fair accuracy (AUC 0.717) only when combined with LV EF, a well-known strong prognostic indicator in inflammatory cardiomyopathy (Sanguineti *et al*, 2015; Spieker *et al*, 2017; Ammirati *et al*, 2018).

On the contrary, the low predictivity of myocardial edema and fibrosis/necrosis extension in our cohort could be explained by the relatively high prevalence of low-grade diffuse myocardial damage (as demonstrated by the elevated percentage of myocardial segments with mapping alterations [41%, 19%, and 44% for native T1, T2, and ECV, respectively], with only mild mean elevation of their values), preventing to build a robust prognostic model. This was the case also for LGE, highly prevalent in our cohort, in agreement with a recent study that found that LGE persists in at least 2/3 of patients after acute myocarditis (Luetkens *et al*, 2016), suggesting that the low detectability of LGE in the chronic setting may be due to scar shrinking and limited spatial resolution of CMR hampering its identification (Eichhorn *et al*, 2022).

However, when evaluating only the patients with significant edema depicted with T2 mapping, we have found that the unique capability of CMR of quantifying the intensity of myocardial alterations, thus the degree of necrosis and edema and the systolic dysfunction, allows for a very good risk stratification, with an AUC of 0.850.

In these patients with active inflammation, the setting is more similar to the acute phase myocarditis, and our results are in agreement with previous literature. In fact, we have found that the most predictive parameters are LV EF, as previously discussed, together with T1 mapping, as found in a previous study on immune checkpoint inhibitor myocarditis (Thavendiranathan *et al*, 2021). T2-ratio was

borderline significant ( $p=0.073$ ), and it could also be associated to a worse prognosis (Spieker *et al*, 2017).

In conclusion, we have found that in consecutive patients with previous myocarditis or suspected chronic active myocarditis, the best parameter to predict prognosis remains the systolic function of the left ventricle, while conventional and novel parametric mapping techniques have a somewhat unsatisfactory capability of risk stratification.

However, in patients with chronic active myocarditis, the capability of CMR of quantifying the degree of inflammation has shown promising results for risk stratification, and could be used to guide tailored therapy (e.g., immunomodulation) and improve patient's outcome.

Limitations of the study are:

- 1) the relatively small number of patients and the retrospective enrollment
- 2) the lack of a validation cohort for the models that we have developed
- 3) the presence of lost at follow-up patients that could introduce bias
- 4) The absence of EMB-confirmation of the entire cohort

This limitations could be overcome by designing future larger multicenter studies with prospective enrollment of patients with a better characterization of inflammation with EMB in a significant number of them.

Future research is needed to improve the parametric mapping techniques, also by introducing whole-heart coverage in order to better capture all the pathophysiological alterations that are induced by inflammation. Furthermore, novel imaging biomarkers such as radiomics, that in acute myocarditis has shown promising results (Baessler *et al*, 2019), could be introduced, along with algorithms of artificial intelligence specifically trained to integrate the multiparametric information derived from CMR to predict prognosis.

## **RESULTS (AIM 2)**

In the study population, no unexpected complications nor any death occurred in the experimental group.

### **CMR experiments**

Among the eight mice of the study group, two underwent only CMR in the chronic phase (40 days after induction), while six underwent CMR both in the acute phase (21 days after induction) and in the chronic phase.

Among the six mice that underwent CMR at both time points, in one the volumes of the acute phase CMR were not evaluable due to artifacts.

In the six mice that underwent CMR at both time points, T1 mapping was evaluated only in the chronic phase; in one of these mice, chronic phase T1 mapping was not evaluable due to artifacts.

The two mice of the control group underwent only non-contrast CMR with evaluation of volumes and function and native T1 mapping.

Thus, the final data comprised volumes and function for seven mice in the acute phase and eight mice in the chronic phase, native and post-contrast T1 mapping for seven mice in the chronic phase, and volumes, function, and native T1 mapping for the two mice of the control group.

EAM of two mice is being processed at time of writing. In three mice, no sufficient quality material was recovered for an informative histological evaluation. In the remaining three mice, histology confirmed myocarditis in two out of three and showed variable extent of replacement fibrosis in three out of three mice.

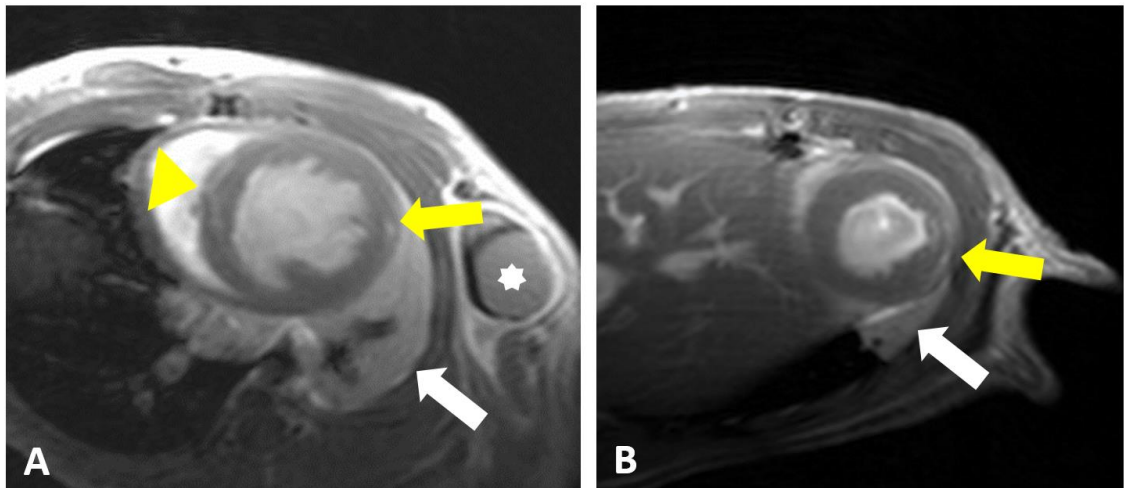
### **Function and LGE**

The mice of the study group had a lower EF than mice of the control group both in the acute (56 [55-58] vs 60 [59-63],  $p=0.036$ ) and chronic phase (54 [51-55] vs 60 [59-63],  $p=0.024$ ).

In the chronic phase, LGE with subepicardial distribution suggestive of non-ischemic cardiomyopathy was found in seven out of eight mice, associated to swollen axillary lymph nodes in all mice and to variable degree of lung atelectasis/pneumonia.

Representative images in figure 5.

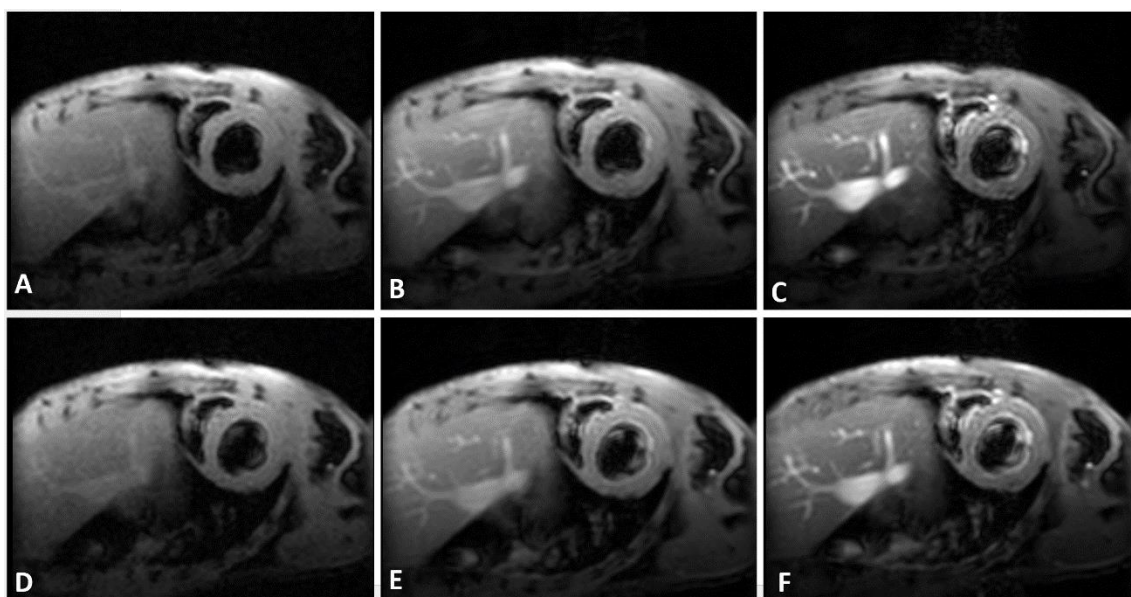
c. On the left (A), CMR images show a mildly dilate LV with evidence of hyperintense areas of LGE in a mesocardial distribution in the mid-ventricular septum (yellow arrowhead) and in a subepicardial distribution on the mid lateral wall (yellow arrow). On the right (B), CMR images show subepicardial areas of LGE in the mid-apical lateral wall (yellow area). On the left (A), asterisk indicates a swollen axillary lymph node. White arrow in A and B indicate areas of consolidated lung parenchyma



### T1 mapping

To obtain native and post-contrast T1 mapping, the same mid ventricular slice was acquired with a cine-IG FLASH sequence varying the flip angle for each acquisition (Figure 6).

Figure 6. Acquisition of VFA cine-IG FLASH sequences. Top row shows pre-contrast cine IG-FLASH images acquired with flip angles of 2° (A), 8° (B), and 14° (C). Bottom row shows pre-contrast cine IG-FLASH images acquired with flip angles of 2° (D), 8° (E), and 14° (F).



Compared to controls, mice with EAM had higher median native T1 values (804 ms [780-863] vs 724 ms [722-725],  $p=0.222$ ). In mice with EAM, T1 significantly decreased after contrast injection (804 ms [780-863] vs 554 ms [443-586],  $p=0.016$ ), as expected. Examples of native and post contrast T1 maps are shown in figure 7 and 8.

Figure 7. Native T1 map. On the left (A) the black and white native T1 map obtained with the VFA approach. On the right (B) the same native T1 map with color coding.

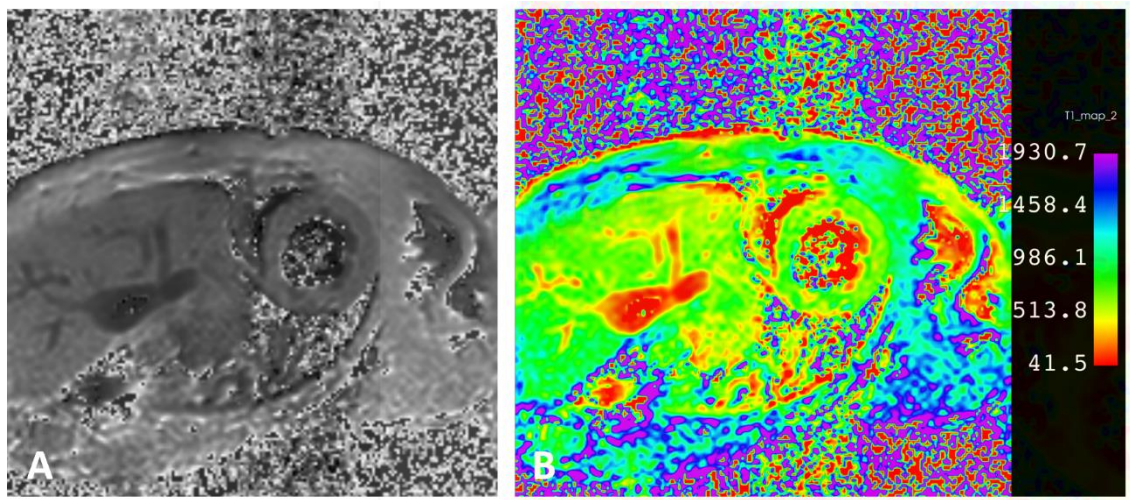
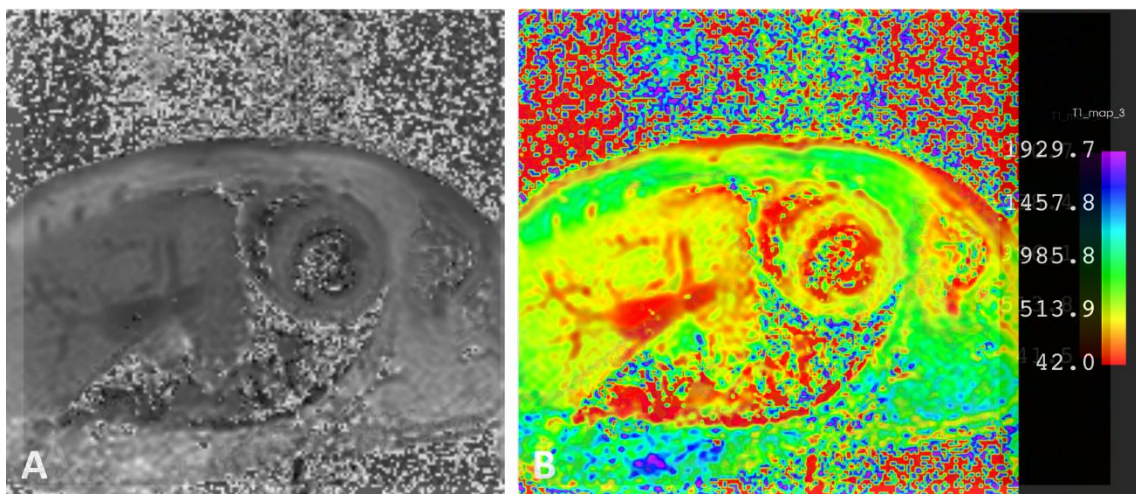


Figure 8. Post-contrast T1 map. On the left (A) the black and white post-contrast T1 map obtained with the VFA approach. On the right (B), the same post-contrast T1 map with color coding.



## **DISCUSSION (AIM 2)**

The main results of our study is the finding that high-field CMR is a feasible modality for the non-invasive evaluation of a preclinical model of experimental autoimmune myocarditis in mice.

In the literature, just a few reports (Błyszczuk, 2019) have studied the application of multiparametric CMR with acquisition of mapping parameters in the setting of experimental myocarditis, but the development of these models is important to prepare preclinical platforms for future testing of pathophysiological hypothesis or novel therapies. Our study goes into this direction by confirming the possibility of using CMR for the monitoring of EAM, especially in this setting characterized by a more subtle and diffuse damage of autoimmune etiology, which closely resembles the clinical setting of chronic myocarditis.

The values of native T1 mapping that we have found (between 700 ms and 900 ms) are in line with a previous study from Coolen et al. (Coolen *et al*, 2011) that have found comparable T1 values in mice when acquiring maps with the VFA method with a black blood approach.

However, the T1 value that we have found is probably underestimated in respect to the true T1 of the tissue, since its dependence on the field strength (Haaf *et al*, 2016). In fact, Coolen et al. (Coolen *et al*, 2011) have found, using a bright blood approach, a T1 value doubled in respect to the black blood approach, probably more adherent to the real T1.

Nevertheless, since we have found that T1 values are different between cases and controls and that T1 mapping significantly decreases after contrast administration, we conclude that this approach is still valuable even if it derives an apparent T1 and not a real T1 value of the tissue.

Limitations on the study are:

- 1) the small number of cases and controls
- 2) the single slice approach that prevents getting information from the whole myocardium
- 3) the lack of histological confirmation in all cases

4) the absence of a method for the evaluation of edema.

However, we are currently developing T2 mapping, using the same VFA approach, by means of DESPOT2 analysis (Deoni et al, 2003), thus we plan to have information also on focal and diffuse edema.

Furthermore, given the availability of both native and post-contrast T1 mapping, we are planning to build ECV maps and to correlate them to the presence and extent of LGE.

Thus, in conclusion, we are still working on the development of a preclinical mice model of autoimmune myocarditis that closely resembles the clinical setting of chronic myocarditis and that can be studied with the same CMR-based multiparametric approach including the evaluation of T1, T2 and ECV mapping.



## **MATERIAL AND METHODS (AIM 1)**

### **Study design and population**

This is a single center retrospective observational study performed according to the principles established in the declaration of Helsinki.

From September 2017 to March 2022, all patients undergoing CMR for clinical suspicion of chronic myocarditis or previous (more than one year) CMR-based diagnosis of myocarditis were screened.

Of the one-hundred and seventy four patients screened, one-hundred and fifty-two fulfilled the following inclusion and exclusion criteria.

### ***Inclusion criteria***

CMR findings of classic myocarditis pattern in a patient with chronic myocarditis suspicion, according to ESC guidelines (Caforio *et al*, 2013), due to presence of:

- a) Symptoms (onset more than one month before CMR (Ammirati *et al*, 2020))
  - i. worsening of dyspnea at rest or exercise, and/or fatigue, with or without left and/or right heart failure signs;
  - ii. palpitation, and/or unexplained arrhythmia symptoms and/or syncope, and/or aborted sudden cardiac death;

**OR** (in asymptomatic patients, one of the following):

- b) ECG/Holter/stress test alterations:
  - i. New findings: atrioventricular block I–III, bundle branch block, ST-segment and T-wave alterations, reduced R wave height, abnormal Q waves, low voltage, sinus arrest, frequent premature beats, supraventricular tachycardia, ventricular tachycardia or fibrillation, and asystole;
- c) Alteration of biomarkers of myocardial injury;

**OR**

- d) Previous CMR-based diagnosis of myocarditis.

### ***Exclusion criteria***

- a) alternative diagnosis explaining symptoms, ECG/Holter/stress test alterations, and alteration of biomarkers of myocardial injury;
- b) history of other cardiomyopathies;
- c) ICD or PM;

- d) myocarditis due to known iatrogenic causes (e.g., immune check-point inhibitor myocarditis).

Eleven patients were excluded due to presence of other cardiac disease and eleven due to myocarditis secondary to known iatrogenic cause, bringing the population to one hundred and fifty-two.

Among these, fifty-nine could not be contacted to collect the follow-up data and were excluded. Thus, the final population included ninety-three patients.

### **CMR acquisition protocol**

CMR was performed on two 1.5 T scanners (Achieva and Achieva dStream, Philips Medical Systems, Eindhoven, The Netherlands) equipped with a 32-channel phased-array coil. Only T2-weighted STIR in short axis plane were acquired with body coil.

The acquisition protocol included the sequences necessary for the evaluation of 2009 (Friedrich *et al*, 2009) and 2018 (Ferreira *et al*, 2018) LLC.

In detail, the protocol included:

- a) Pre-contrast cine steady state free precession (SSFP) sequences in long-axis 2-chamber, 3-chambers, and 4-chambers planes;
- b) T2-weighted STIR sequences in long-axis 2-chamber, 3-chambers, and 4-chambers planes and in short-axis covering the entire left ventricle (LV);
- c) Native T1 mapping using a modified Look-Locker inversion recovery (MOLLI) sequence with 5(3)3 sampling scheme (Messroghli *et al*, 2004);
- d) T2 mapping using a gradient-(echo planar imaging) and spin-echo multi-echo sequence (GraSE) (Sprinkart *et al*, 2015);
- e) Post-contrast (three minutes after contrast media injection) cine steady-state free precession (ce-SSFP) sequence covering the entire LV for evaluation of morphology and function of left and right ventricles;
- f) Post-contrast (ten minutes after contrast media injection) Late Gadolinium Enhancement (LGE) sequence in long-axis 2-chamber, 3-chambers, and 4-chambers planes and in short-axis, covering the entire left ventricle (LV);
- g) Post-contrast T1 mapping using a modified Look-Locker inversion recovery sequence with a 4(1)3(1)2 sampling scheme (Haaf *et al*, 2016).

Native-T1, T2, and post-contrast T1 mapping were acquired in three short axis slices (basal, mid-ventricular, and apical).

Contrast media (0.15 mmol/kg of gadobutrol [Gadovist; Bayer Healthcare, Berlin, Germany]) was automatically injected from an antecubital vein of the right arm, followed by a saline flush (20 mL at 3.5 mL/s).

### **CMR analysis**

CMR examinations were analyzed by an experienced reader using dedicated software (cvi42 5.11, Circle Cardiovascular Imaging, Calgary, Canada).

LV and RV end-diastolic volumes (LV-EDV; RV-EDV) and end-systolic volumes (LV-ESV; RV-ESV), ejection fraction (LVEF and RVEF), and LV end-diastolic wall mass (LV-EDWM) were obtained automatically after drawing the epicardial and endocardial contours in the end-diastolic and end-systolic short-axis SSFP images.

Myocardial edema was qualitatively assessed on T2-weighted STIR images as areas of myocardial hyperintensity, and semi-quantitatively as the ratio between myocardial and skeletal muscle signal intensity (SI) (T2-ratio, positive when  $\geq 1.9$ ) (Friedrich *et al*, 2009).

Myocardial fibrosis/necrosis were qualitatively assessed on LGE images as areas of myocardial hyperintensity with non-ischemic pattern (subepicardial or mesocardial distribution), and semi-quantitatively as percentage of injured myocardium (scar burden) with a mean signal intensity 5 times the standard deviation (SD) of the mean signal intensity of the remote myocardium, after drawing the endocardial and epicardial border of LV on LGE images (Schulz-Menger *et al*, 2020).

T2, native-T1 and post-contrast T1 values were extracted by drawing endocardial and epicardial borders on the three short-axis (basal, mid-ventricular, and apical) slices. To minimize partial volume effects of blood and fat, an automatic offset of 10% from endocardial and epicardial borders was set.

Extracellular volume fraction (ECV) was calculated as the ratio between the relaxivity of myocardium and blood pool before and after contrast media administration, pondered for the hematocrit, according to the following formula:

$$ECV = hct \times \frac{R1_{postcontrast\ myocardium} - R1_{native\ myocardium}}{R1_{postcontrast\ blood\ pool} - R1_{native\ blood\ pool}}$$

where R1 is equal to the relaxation rate (1/T1).

Each CMR parameter was evaluated according to the American Heart Association (AHA) 16-segment model (Cerqueira *et al*, 2002).

To avoid biases due to the variable number of unevaluable segments in each patient, the percentage of altered segments for each mapping parameter has been used instead of the absolute number of altered segments.

### **Endomyocardial biopsy and histological analysis**

EMB was performed from the ventricular septum (4-6 samples for each patient) under fluoroscopic and transthoracic echocardiogram guidance, accessing from the jugular vein. The samples were analyzed at a tertiary referral center (University of Padua). The histological diagnosis of myocarditis was based on the Dallas criteria, which establish the diagnosis in the presence of lymphocyte and/or macrophage count  $> 14/\text{mm}^2$  (Basso *et al*, 2013). Immunohistochemistry using antibodies against CD3, CD43, CD20, and CD68 was performed to characterize inflammatory infiltrates. A standard panel of 15 viruses was analyzed by polymerase chain reaction (PCR).

### **Study endpoint**

After a median follow-up of 21 (IQR, 17-35) months from CMR, we collected a composite outcome derived from the occurrence of:

- cardiovascular death;
- chronic heart failure, defined as symptoms and/or signs of HF caused by a structural and/or functional cardiac abnormality with at least one between:
  - elevated NT-proBNP ( $>125$  pg/mL);
  - objective evidence of cardiogenic pulmonary or systemic congestion (Bozkurt *et al*, 2021);
- Hospitalization for cardiac reasons
- Recurrent chronic myocarditic chest pain;
- ICD/PM implantation;
- Arrhythmias, defined as non-sustained ventricular tachycardia (NSVT), sustained ventricular tachycardia (SVT), ventricular fibrillation (VF), atrioventricular (AV) block  $\geq$  grade 2, premature ventricular complexes (PVCs)  $\geq$  grade 2 according to Lown classification (Bastiaenen *et al*, 2012), found at outpatient ECG, Holter ECG monitoring, or after loop recorder implantation.

Follow-up data were obtained with telehealth or in-person medical visits.

### **Statistical analysis**

Continuous variables are reported as mean±SD if normally distributed and as median and interquartile range (IQR) in case of not normal distribution. Categorical variables are reported as absolute numbers and percentages.

Comparisons between groups were performed with chi-square test, Fisher's exact test, unpaired-sample T Test, or Mann–Whitney U test, according to variable type and distribution.

The receiver operating characteristic (ROC) curves were computed to analyze the performance of the models in predicting the composite outcome. The area under the receiver operating characteristic curve (AUC), with 95% confidence intervals, was computed to compare the predicting capabilities of the models. AUC values >0.80 were considered very good, between 0.70 and 0.80 as good, between 0.6 and 0.69 as acceptable, <0.6 as poor. AUCs were compared as recommended by DeLong et al. (DeLong *et al*, 1988).

All tests were two-tailed. A p value of less than .05 was required for statistical significance. All calculations were computed using the "Statistical Analysis System" software (SAS version 9.4; SAS Institute).

## **MATERIAL AND METHODS (AIM 2)**

### **Study design**

The study was conducted according to the principles of the Italian Ministry of Health guidelines for the use and care of experimental animals.

Eight male C57BL/6N mice (Charles River Laboratories Italia, Italy), 6-8 weeks old, underwent experimental autoimmune myocarditis (EAM) induction and composed the study group. Two mice composed the control group.

Mice from the study group underwent induction at time 0, the first CMR in the acute phase of myocarditis after  $22 \pm 2$  days, the second CMR in the chronic phase of myocarditis at  $35 \pm 2$  days, and histopathological evaluation at day  $104 \pm 21$ .

Mice from the control group underwent CMR at a single time point and subsequent histopathological evaluation.

### **Experimental autoimmune myocarditis induction**

To induce the EAM, animals received a subcutaneous injection of 150  $\mu$ g of  $\alpha$ -MyHC peptide emulsified in a 1:1 ratio with complete Freund's adjuvant (CFA), after a mild anesthesia induced by isoflurane at a concentration of 1-2% through the Vevo<sup>TM</sup> Compact Anesthesia System. In the animals of the control group, a sham subcutaneous injection of 150  $\mu$ g of CFA was performed.

### **CMR acquisition protocol**

CMR examinations were performed on a 7 T preclinical scanner (Bruker, BioSpec 70/30 USR, Paravision 6.0), equipped with 450/675 mT/m gradients (slew-rate: 3400–4500 T/m/s; rise-time 140  $\mu$ s) and 400 MHz cryogenic radiofrequency (RF) surface coil.

All mice were subjected to general anesthesia with isoflurane (3% for induction and 2% for maintenance in 2 L/min of oxygen). During CMR, body temperature and respiratory rate were monitored (SA Instruments, Inc., Stony Brook, NY, USA) and maintained around 37 °C and 30 breaths-per-minute, respectively.

The CMR protocol was composed of a pre-contrast long axis 2-chamber and 4-chambers 2D-intrigated (IG) cine fast low-angle shot (FLASH) sequence (TR = 8 ms, TE = 2.5 ms; field of view = 26 × 18 mm, slice thickness = 1 mm, spatial resolution = 0.102 × 0.070 mm/pixel; cardiac phases = 30).

These sequences were used to plan the acquisition of a single mid-ventricular slice acquired as a 2D-IG cine FLASH sequence with the following parameters: (TR = 12 ms, TE = 2.5 ms, FA = 2°; field of view = 26 × 18 mm, slice thickness = 1 mm, spatial resolution = 0.102 × 0.070 mm/pixel; cardiac phases = 12). The same sequence was repeated two other times, at the same position, by changing the FA to 8° and 14°, to determine the T1 relaxation time of myocardium with DESPOT1 analysis. The sequences at FA 2°, 8°, and 14° were repeated at the same location after contrast injection to determine the post-contrast T1 value of myocardium.

After ten minutes from the injection of 0.15 mmol/kg of gadobutrol (Gadovist, Bayer Healthcare, Berlin, Germany) at 300 µl/min flow rate, a short-axis 2D-IG cine FLASH sequence, with the same parameters as previously described, acquired from the apex to the base, was performed to evaluate LV volumes and function and to assess the presence of hyperintense stripe compatible with LGE.

### **CMR analysis**

CMR examinations were analyzed by an experienced reader using dedicated software (cvi42 5.11, Circle Cardiovascular Imaging, Calgary, Canada).

LV and RV end-diastolic volumes (LV-EDV; RV-EDV) and end-systolic volumes (LV-ESV; RV-ESV), ejection fraction (LVEF and RVEF), and LV end-diastolic wall mass (LV-EDWM) were obtained after manually drawing the epicardial and endocardial contours in the end-diastolic and end-systolic short-axis cine images.

Myocardial fibrosis/necrosis were qualitatively assessed on cine images as areas of myocardial hyperintensity with non-ischemic pattern (subepicardial or mesocardial distribution).

### **T1 quantification**

Pre- and post-contrast T1 of the myocardium has been quantified using DESPOT1 analysis (Deoni *et al*, 2003; Coolen *et al*, 2011).

The basis of this technique relies on the dependence of the steady-state (SS) radiofrequency (RF)-spoiled gradient echo signal to the FA of the sequence. Using the linearized form of the Ernst equation [1] it is possible, from SS signal, to derive the T1 and the proton density ( $M_0$ ) of the image.

$$\frac{M^{SS}}{\sin(\alpha)} = e^{-TR/T_1} \frac{M^{SS}}{\tan(\alpha)} + M_0(1 - e^{-TR/T_1}) \quad [1]$$

In this equation,  $M^{SS}$  is the steady-state signal, measured in arbitrary units (AU), TR is the repetition time of the sequence (12 ms), and  $\alpha$  is the flip angle (2°, 8°, and 14° in our sequences).

In this linearized form,  $e^{-TR/T_1}$  is the slope while  $M_0(1 - e^{-TR/T_1})$  is the intercept of the equation. Thus, using a fitting algorithm in a pixel-wise approach, we were able to create native and post-contrast T1 maps.

To quantify the T1 value of the myocardium, T1 maps were segmented using 3D Slicer (<https://www.slicer.org/>).

### **Histopathological analysis**

Analysis has been carried as previously described (Palmisano *et al*, 2020). In brief, after sacrifice the mice left ventricle was perfused with PBS pH 7.5, followed by 10% buffered formalin. After, the hearts were harvested, fixed, and paraffin-included, cutting in thin sections, and then stained with hematoxylin/eosin for the morphological analyses.



## REFERENCES

- Ammann P, Naegeli B, Schuiki E, Straumann E, Frielingsdorf J, Rickli H & Bertel O (2003) Long-term outcome of acute myocarditis is independent of cardiac enzyme release. *Int J Cardiol* 89: 217–222
- Ammirati E, Cipriani M, Moro C, Raineri C, Pini D, Sormani P, Mantovani R, Varrenti M, Pedrotti P, Conca C, *et al* (2018) Clinical Presentation and Outcome in a Contemporary Cohort of Patients With Acute Myocarditis: Multicenter Lombardy Registry. *Circulation* 138: 1088–1099
- Ammirati E, Frigerio M, Adler ED, Basso C, Birnie DH, Brambatti M, Friedrich MG, Klingel K, Lehtonen J, Moselehi JJ, *et al* (2020) Management of Acute Myocarditis and Chronic Inflammatory Cardiomyopathy. *Circ Hear Fail* 13: E007405
- Anzini M, Merlo M, Artico J & Sinagra G (2016) Arrhythmic risk prediction of acute myocarditis presenting with life-threatening ventricular tachyarrhythmias. *Int J Cardiol* 212: 169–170
- Aquaro GD, Perfetti M, Camastra G, Monti L, Dellegrottaglie S, Moro C, Pepe A, Todiere G, Lanzillo C, Scatteia A, *et al* (2017) Cardiac MR With Late Gadolinium Enhancement in Acute Myocarditis With Preserved Systolic Function: ITAMY Study. *J Am Coll Cardiol* 70: 1977–1987
- Arbelo E, Protonotarios A, Gimeno JR, Arbustini E, Barriales-Villa R, Basso C, Bezzina CR, Biagini E, Blom NA, de Boer RA, *et al* (2023) 2023 ESC Guidelines for the management of cardiomyopathies. *Eur Heart J* 44: 3503–3626
- Aretz HT (1987) Myocarditis: the Dallas criteria. *Hum Pathol* 18: 619–624
- Baessler B, Luecke C, Lurz J, Klingel K, Das A, Von Roeder M, De Waha-Thiele S, Besler C, Rommel KP, Maintz D, *et al* (2019) Cardiac MRI and texture analysis of myocardial T1 and T2 maps in myocarditis with acute versus chronic symptoms of heart failure. *Radiology*

292: 608–617

- Basso C, Calabrese F, Angelini A, Carturan E & Thiene G (2013) Classification and histological, immunohistochemical, and molecular diagnosis of inflammatory myocardial disease. *Heart Fail Rev* 18: 673–681
- Basso C, Calabrese F, Corrado D & Thiene G (2001) Postmortem diagnosis in sudden cardiac death victims: macroscopic, microscopic and molecular findings. *Cardiovasc Res* 50: 290–300
- Bastiaenen R, Batchvarov V & Gallagher MM (2012) Ventricular automaticity as a predictor of sudden death in ischaemic heart disease. *Europace* 14: 795–803
- Bennett MK, Gilotra NA, Harrington C, Rao S, Dunn JM, Freitag TB, Halushka MK & Russell SD (2013) Evaluation of the role of endomyocardial biopsy in 851 patients with unexplained heart failure from 2000-2009. *Circ Heart Fail* 6: 676–684
- Błyszczuk P (2019) Myocarditis in Humans and in Experimental Animal Models. *Front Cardiovasc Med* 6: 64
- Bohnen S, Radunski UK, Lund GK, Ojeda F, Looft Y, Senel M, Radziwolek L, Avanesov M, Tahir E, Stehning C, *et al* (2017) Tissue characterization by T1 and T2 mapping cardiovascular magnetic resonance imaging to monitor myocardial inflammation in healing myocarditis. *Eur Hear J - Cardiovasc Imaging* 18: 744–751
- Bozkurt B, Coats AJ, Tsutsui H, Abdelhamid M, Adamopoulos S, Albert N, Anker SD, Atherton J, Böhm M, Butler J, *et al* (2021) Universal Definition and Classification of Heart Failure: A Report of the Heart Failure Society of America, Heart Failure Association of the European Society of Cardiology, Japanese Heart Failure Society and Writing Committee of the Universal Definition . *J Card Fail*
- Caforio ALP, Adler Y, Agostini C, Allanore Y, Anastasakis A, Arad M, Böhm M, Charron P, Elliott PM, Eriksson U, *et al* (2017) Diagnosis and management of myocardial involvement in systemic immune-

- mediated diseases: a position statement of the European Society of Cardiology Working Group on Myocardial and Pericardial Disease. *Eur Heart J* 38: 2649–2662
- Caforio ALP, Pankuweit S, Arbustini E, Basso C, Gimeno-Blanes J, Felix SB, Fu M, Heliö T, Heymans S, Jahns R, *et al* (2013) Current state of knowledge on aetiology, diagnosis, management, and therapy of myocarditis: A position statement of the European Society of Cardiology Working Group on Myocardial and Pericardial Diseases. *Eur Heart J* 34: 2636–2648
- Cerqueira MD, Weissman NJ, Dilsizian V, Jacobs AK, Kaul S, Laskey WK, Pennell DJ, Rumberger JA, Ryan T & Verani MS (2002) Standardized myocardial segmentation and nomenclature for tomographic imaging of the heart: A Statement for Healthcare Professionals from the Cardiac Imaging Committee of the Council on Clinical Cardiology of the American Heart Association. *Circulation* 105: 539–542 doi:10.1161/hc0402.102975 [PREPRINT]
- Coolen BF, Geelen T, Paulis LEM, Nauerth A, Nicolay K & Strijkers GJ (2011) Three-dimensional T1 mapping of the mouse heart using variable flip angle steady-state MR imaging. *NMR Biomed* 24: 154–162
- Cooper LT (2009) Myocarditis. *N Engl J Med* 360: 1526–1538
- Cooper LTJ & Fairweather D (2013) We see only what we look for: imaging cardiac inflammation. *Circ Cardiovasc Imaging* 6: 165–166 doi:10.1161/CIRCIMAGING.113.000166 [PREPRINT]
- Corrado D, Basso C & Thiene G (2001) Sudden cardiac death in young people with apparently normal heart. *Cardiovasc Res* 50: 399–408
- DeLong ER, DeLong DM & Clarke-Pearson DL (1988) Comparing the Areas under Two or More Correlated Receiver Operating Characteristic Curves: A Nonparametric Approach. *Biometrics* 44: 837

- Deoni SCL, Rutt BK & Peters TM (2003) Rapid combined T1 and T2 mapping using gradient recalled acquisition in the steady state. *Magn Reson Med* 49: 515–526
- Eckart RE, Shry EA, Burke AP, McNear JA, Appel DA, Castillo-Rojas LM, Avedissian L, Pearse LA, Potter RN, Tremaine L, *et al* (2011) Sudden death in young adults: an autopsy-based series of a population undergoing active surveillance. *J Am Coll Cardiol* 58: 1254–1261
- Eichhorn C, Greulich S, Bucciarelli-Ducci C, Sznitman R, Kwong RY & Gräni C (2022) Multiparametric Cardiovascular Magnetic Resonance Approach in Diagnosing, Monitoring, and Prognostication of Myocarditis. *JACC Cardiovasc Imaging* 15: 1325–1338
- Esposito A, Francone M, Faletti R, Centonze M, Cademartiri F, Carbone I, De Rosa R, Di Cesare E, La Grutta L, Ligabue G, *et al* (2016) Lights and shadows of cardiac magnetic resonance imaging in acute myocarditis. *Insights Imaging* 7: 99–110
- Felker GM, Hu W, Hare JM, Hruban RH, Baughman KL & Kasper EK (1999) The spectrum of dilated cardiomyopathy. The Johns Hopkins experience with 1,278 patients. *Medicine (Baltimore)* 78: 270–283
- Ferreira VM, Schulz-Menger J, Holmvang G, Kramer CM, Carbone I, Sechtem U, Kindermann I, Gutberlet M, Cooper LT, Liu P, *et al* (2018) Cardiovascular Magnetic Resonance in Nonischemic Myocardial Inflammation: Expert Recommendations. *J Am Coll Cardiol* 72: 3158–3176
- Friedrich MG, Sechtem U, Schulz-Menger J, Holmvang G, Alakija P, Cooper LT, White JA, Abdel-Aty H, Gutberlet M, Prasad S, *et al* (2009) Cardiovascular Magnetic Resonance in Myocarditis: A JACC White Paper. *J Am Coll Cardiol* 53: 1475–1487 doi:10.1016/j.jacc.2009.02.007 [PREPRINT]

- Gräni C, Eichhorn C, Bière L, Murthy VL, Agarwal V, Kaneko K, Cuddy S, Aghayev A, Steigner M, Blankstein R, *et al* (2017) Prognostic Value of Cardiac Magnetic Resonance Tissue Characterization in Risk Stratifying Patients With Suspected Myocarditis. *J Am Coll Cardiol* 70: 1964–1976
- Greulich S, Seitz A, Müller KAL, Grün S, Ong P, Ebadi N, Kreisselmeier KP, Seizer P, Bekeredjian R, Zwadlo C, *et al* (2020) Predictors of Mortality in Patients With Biopsy-Proven Viral Myocarditis: 10-Year Outcome Data. *J Am Heart Assoc* 9: e015351
- Grün S, Schumm J, Greulich S, Wagner A, Schneider S, Bruder O, Kispert E-M, Hill S, Ong P, Klingel K, *et al* (2012) Long-term follow-up of biopsy-proven viral myocarditis: predictors of mortality and incomplete recovery. *J Am Coll Cardiol* 59: 1604–1615
- Guidelines for diagnosis and treatment of myocarditis (JCS 2009): digest version. (2011) *Circ J* 75: 734–743
- Haaf P, Garg P, Messroghli DR, Broadbent DA, Greenwood JP & Plein S (2016) Cardiac T1 Mapping and Extracellular Volume (ECV) in clinical practice: A comprehensive review. *J Cardiovasc Magn Reson* 18: 89
- Hinojar R, Foote L, Ucar EA, Jackson T, Jabbour A, Yu CY, McCrohon J, Higgins DM, Carr-White G, Mayr M, *et al* (2015) Native T1 in discrimination of acute and convalescent stages in patients with clinical diagnosis of myocarditis: A proposed diagnostic algorithm using CMR. *JACC Cardiovasc Imaging* 8: 37–46
- Imazio M & Trinchero R (2008) Myopericarditis: Etiology, management, and prognosis. *Int J Cardiol* 127: 17–26
- Kindermann I, Kindermann M, Kandolf R, Klingel K, Bültmann B, Müller T, Lindinger A & Böhm M (2008) Predictors of outcome in patients with suspected myocarditis. *Circulation* 118: 639–648
- Kueth F, Franz M, Jung C, Pörrmann C, Reinbothe F, Schlattmann P, Egerer R & Mall G (2017) Outcome predictors in dilated

- cardiomyopathy or myocarditis. *Eur J Clin Invest* 47: 513–523
- Lagan J, Schmitt M & Miller CA (2018) Clinical applications of multi-parametric CMR in myocarditis and systemic inflammatory diseases. *Int J Cardiovasc Imaging* 34: 35–54
- De Luca G, Campochiaro C, Sartorelli S, Peretto G & Dagna L (2020) Therapeutic strategies for virus-negative myocarditis: a comprehensive review. *Eur J Intern Med* 77: 9–17 doi:10.1016/j.ejim.2020.04.050 [PREPRINT]
- Luetkens JA, Faron A, Isaak A, Dabir D, Kuetting D, Feisst A, Schmeel FC, Sprinkart AM & Thomas D (2019) Comparison of Original and 2018 Lake Louise Criteria for Diagnosis of Acute Myocarditis: Results of a Validation Cohort. *Radiol Cardiothorac imaging* 1: e190010
- Luetkens JA, Homsí R, Dabir D, Kuetting DL, Marx C, Doerner J, Schlesinger-Irsch U, Andrié R, Sprinkart AM, Schmeel FC, *et al* (2016) Comprehensive Cardiac Magnetic Resonance for Short-Term Follow-Up in Acute Myocarditis. *J Am Heart Assoc* 5: e003603
- Lurz P, Luecke C, Eitel I, Föhrenbach F, Frank C, Grothoff M, de Waha S, Rommel K-P, Lurz JA, Klingel K, *et al* (2016) Comprehensive Cardiac Magnetic Resonance Imaging in Patients With Suspected Myocarditis: The MyoRacer-Trial. *J Am Coll Cardiol* 67: 1800–1811
- Maron BJ, Udelson JE, Bonow RO, Nishimura RA, Ackerman MJ, Estes NAM, Cooper LT, Link MS & Maron MS (2015) Eligibility and Disqualification Recommendations for Competitive Athletes With Cardiovascular Abnormalities: Task Force 3: Hypertrophic Cardiomyopathy, Arrhythmogenic Right Ventricular Cardiomyopathy and Other Cardiomyopathies, and Myocarditis: A Scientific Statement. *J Am Coll Cardiol* 66: 2362–2371
- Messroghli DR, Radjenovic A, Kozerke S, Higgins DM, Sivananthan MU & Ridgway JP (2004) Modified Look-Locker inversion recovery (MOLLI) for high-resolution T1 mapping of the heart. *Magn Reson*

- Med* 52: 141–146
- Palmisano A, Piccoli M, Monti CB, Canu T, Cirillo F, Napolitano A, Perani L, Signorelli P, Vignale D, Anastasia L, *et al* (2020) Single-shot morpho-functional and structural characterization of the left-ventricle in a mouse model of acute ischemia-reperfusion injury with an optimized 3D IntraGate cine FLASH sequence at 7T MR. *Magn Reson Imaging* 68: 127–135
- Peretto G, Sala S, Rizzo S, Palmisano A, Esposito A, De Cobelli F, Campochiaro C, De Luca G, Foppoli L, Dagna L, *et al* (2020) Ventricular Arrhythmias in Myocarditis: Characterization and Relationships With Myocardial Inflammation. *J Am Coll Cardiol* 75: 1046–1057
- Petersen SE, Aung N, Sanghvi MM, Zemrak F, Fung K, Paiva JM, Francis JM, Khanji MY, Lukaschuk E, Lee AM, *et al* (2017) Reference ranges for cardiac structure and function using cardiovascular magnetic resonance (CMR) in Caucasians from the UK Biobank population cohort. *J Cardiovasc Magn Reson Off J Soc Cardiovasc Magn Reson* 19: 18
- Radunski UK, Lund GK, Säring D, Bohnen S, Stehning C, Schnackenburg B, Avanesov M, Tahir E, Adam G, Blankenberg S, *et al* (2017) T1 and T2 mapping cardiovascular magnetic resonance imaging techniques reveal unapparent myocardial injury in patients with myocarditis. *Clin Res Cardiol* 106: 10–17
- Roth GA, Mensah GA, Johnson CO, Addolorato G, Ammirati E, Baddour LM, Barengo NC, Beaton AZ, Benjamin EJ, Benziger CP, *et al* (2020) Global Burden of Cardiovascular Diseases and Risk Factors, 1990–2019: Update From the GBD 2019 Study. *J Am Coll Cardiol* 76: 2982–3021
- Sagar S, Liu PP & Cooper LTJ (2012) Myocarditis. *Lancet (London, England)* 379: 738–747
- Sanguineti F, Garot P, Mana M, O'h-Ici D, Hovasse T, Unterseeht T,

- Louvard Y, Troussier X, Morice M-C & Garot J (2015) Cardiovascular magnetic resonance predictors of clinical outcome in patients with suspected acute myocarditis. *J Cardiovasc Magn Reson Off J Soc Cardiovasc Magn Reson* 17: 78
- Schulz-Menger J, Bluemke DA, Bremerich J, Flamm SD, Fogel MA, Friedrich MG, Kim RJ, Von Knobelsdorff-Brenkenhoff F, Kramer CM, Pennell DJ, *et al* (2020) Standardized image interpretation and post-processing in cardiovascular magnetic resonance - 2020 update: Society for Cardiovascular Magnetic Resonance (SCMR): Board of Trustees Task Force on Standardized Post-Processing. *J Cardiovasc Magn Reson* 22 doi:10.1186/s12968-020-00610-6 [PREPRINT]
- Spieker M, Haberkorn S, Gastl M, Behm P, Katsianos S, Horn P, Jacoby C, Schnackenburg B, Reinecke P, Kelm M, *et al* (2017) Abnormal T2 mapping cardiovascular magnetic resonance correlates with adverse clinical outcome in patients with suspected acute myocarditis. *J Cardiovasc Magn Reson Off J Soc Cardiovasc Magn Reson* 19: 38
- Sprinkart AM, Luetkens JA, Träber F, Doerner J, Gieseke J, Schnackenburg B, Schmitz G, Thomas D, Homsy R, Block W, *et al* (2015) Gradient Spin Echo (GraSE) imaging for fast myocardial T2 mapping. *J Cardiovasc Magn Reson* 17: 1–9
- Thavendiranathan P, Zhang L, Zafar A, Drobni ZD, Mahmood SS, Cabral M, Awadalla M, Nohria A, Zlotoff DA, Thuny F, *et al* (2021) Myocardial T1 and T2 Mapping by Magnetic Resonance in Patients With Immune Checkpoint Inhibitor-Associated Myocarditis. *J Am Coll Cardiol* 77: 1503–1516
- Towbin JA, Lowe AM, Colan SD, Sleeper LA, Orav EJ, Clunie S, Messere J, Cox GF, Lurie PR, Hsu D, *et al* (2006) Incidence, causes, and outcomes of dilated cardiomyopathy in children. *JAMA* 296: 1867–1876



Tschöpe C, Ammirati E, Bozkurt B, Caforio ALP, Cooper LT, Felix SB, Hare JM, Heidecker B, Heymans S, Hübner N, *et al* (2021) Myocarditis and inflammatory cardiomyopathy: current evidence and future directions. *Nat Rev Cardiol* 18: 169–193 doi:10.1038/s41569-020-00435-x [PREPRINT]

A handwritten signature in black ink, appearing to be 'AM' or similar initials, located on the right side of the page.